CONTRACT SERIAL NUMBER 1SQ 85-00099
DSS REQUISITION NUMBER 23440-5-9032
CONTRACTOR: C&M Engineering Ltd.

Report No. 57-10480
Contract No. 035Q-233440-5-9032

EFFECT OF CO_2 ON SEAMLESS AND TUBULAR GOODS

for
C & M Engineering Ltd.
2220 - 39th Ave. N.E.
Calgary, Alberta
T2E 6P7

Attention: Mr. Colin Duncan

Prepared by:
J. D. Tyrer, Ph.D.
S. H. Lo, Ph.D.
R. T. Lassau, Head Materials Corrosion/
Metals Investigations

January 27, 1987

11 pp

MICROMEDIA

ONTARIO RESEARCH FOUNDATION
SHERIDAN PARK RESEARCH COMMUNITY
MISSISSAUGA, ONTARIO, CANADA, L5K 1B3
(416) 822-4111 * TELEX 06-982311

EXECUTIVE SUMMARY

The purpose of this study was to investigate the corrosion resistance to high temperature (100°C - 150°C) CO_2 brine solutions of seamless and ERW downhole tubular carbon steels provided by Algoma Steel, (Sault Ste. Marie, Ontario) and IPSCO, (Regina, Saskatchewan). The study indicated that corrosion was minimal (< 0.5mm) for all steel grades in the 100°C - 150°C temperature range. Briefly, corrosion attack was uniform with no evidence of selective microstructural attack. The ERW samples showed no evidence of excessive corrosion attack at the weld or heat affected zones. Minimal corrosion of all steel grades was due in part to the formation of a hard, crystalline impermeable siderite, $FeCO_3$, film on the metal surface. The presence of this film protected the steel surfaces from further corrosion. In addition, it was demonstrated that sodium bicarbonate, $NaHCO_3$, and calcium chloride, $CaCl_2$, can potentially inhibit corrosion in aqueous CO_2/brine solutions. It is suggested that a program be developed to determine the ability of $NaHCO_3$ and $CaCl_2$ to inhibit corrosion of carbon steel materials in H_2S/CO_2 brine solutions.

SOMMAIRE EXÉCUTIF

L'objet de cette étude était pour examiner la résistance de corrosion des aciers de carbone tubulaires sans soudure et de puits de pétrole et du gaz, soudés par la résistance électrique (ERW) aux solutions saumures de CO_2 à haute température (100 - 150°C). Les tuyautages étaient fournis par Algoma Steel, (Sault Ste. Marie, Ontario) et IPSCO, (Regina, Saskatchewan).

Cette étude indiquait que la corrosion étaient minimum (< 0.5 mm) pour toutes les teneurs d'acier aux températures entre 100 et 150°C. En quelques mots, l'attaque de la corrosion était uniforme sans évidence d'attaque sélectif microstructural. Les prélèvements d'ERW ne montraient pas d'évidence d'attaque extrême de la corrosion aux zones de soudure ou aux zones touchées par la chaleur. La corrosion minimum de toutes les teneurs d'acier s'explique, en partie, par la formation d'une couche dure, crystalline et imperméable de sidérite, $FeCO_3$, sur la surface métalique. La présence de cette couche protégeait les surfaces de l'acier de plus de corrosion. En addition, il était démonstré que le bicarbonate de soude, $NaHCO_3$, et le chlorure de calcium, $CaCl_2$, pourraient inhiber virtuellement la corrosion dans les solutions d'aqueux de CO_2/saumure. On propose le développement d'un programme pour déterminer la capacité de $NaHCO_3$ et de $CaCl_2$ pour inhiber la corrosion des matériaux d'acier de carbone dans les solutions de H_2S/CO_2 saumure.

TABLE OF CONTENTS

		Pg. #
	EXECUTIVE SUMMARY	(i)
	RESUME	
	TABLE OF CONTENTS	
	LIST OF TABLES	
	LIST OF FIGURES	
1.	INTRODUCTION	1
2.	OBJECTIVES	1
3.	PROCEDURES	2
	3.1 Autoclave System	2
	3.2 Experimental Procedure	2
	3.3 Coupon Preparation	4
	3.4 X-ray Diffraction Analysis	5
	3.5 Corrosion Rates	6
	3.6 Variation in the Corrosion Rates of Coupons of the Same Steel Grade Exposed to a Chemical Environment	7
	3.7 Metallography	9
4.	RESULTS AND DISCUSSION	10
	4.1 Corrosion Rate Data for Coupons Exposed to a 150°C, 50% CO_2 4,000 psi/Brine Solution, Test Run #1 and #3	10
	4.2 Corrosion Rate Data for Coupons Exposed to a 100°C, 50% CO_2 4,000 psi/Brine Solution, Test Run #4	11
	4.3 Corrosion Rate Data for Coupons Exposed to a 150°C, Brine Solution, (Total Pressure 4,000 psi N_2), Test Test Run #2	11

Pg. #

4.4 Corrosion Rate Data for Coupons Exposed to a 150°C, 50% CO_2 4,000 psi/Brine Solution Test Run #5, Note $NaHCO_3$ and $CaCl_2$ components of the Brine were replaced with NaCl) 12

4.5 Discussion of Corrosion Rate Data 12

4.6 Results of Metallographic Examination - Test Run #1 16

4.6.1 Test Run #1

4.6.2 Test Run #2

4.6.3 Test Run #3

4.6.4 Test Run #4

4.6.5 Test Run #5

5. SUMMARY AND CONCLUSIONS 19

6. COMPARISON OF CORROSION RATES FROM LABORATORY AND FIELD STUDIES 21

7. FUTURE STUDIES 22

BIBLIOGRAPHY

APPENDIX A
Mounting Configuration of Carbon Steel Coupons on Teflon Coupon Rack 57

LIST OF TABLES

	Page
TABLE 1 Chemical Compositions of Test Materials	24
TABLE 2 Brine Composition (ASTM - D1141)	24
TABLE 3 Autoclave Experiment	26
TABLE 4 Corrosion Rate Data for K-55 Seamless Specimens	27
TABLE 5 Corrosion Rate Data for L-80 Seamless Specimens	28
TABLE 6 Corrosion Rate Data for S0095 Seamless Specimens	29
TABLE 7 Corrosion Rate DAta for IJW-55 ERW Specimens	30
TABLE 8 Corrosion Rate Data for IKW-55 ERW Specimens	31
TABLE 9 Corrosion Rate Data for ILW-80 ERW Specimens	32

List of Tables continued.....

TABLE 10
Average Corrosion Rates (mm/yr) and 90% Confidence Limit Calculator from ± Distribution 33

TABLE 11
Ratio of the Average Corrosion Rates for Experiment Numbers 3 and 5 34

TABLE 12
Correlation of Corrosion Resistance and Corrosion Rate 35

TABLE 13
Results of Metallographic Examination of Algoma Steels 36

TABLE 14
Results of Metallographic Examination of Ipsco Steels 37

TABLE 15
Results of Metallographic Examination 38

TABLE 16
Results of Metallographic Examination 39

TABLE 17
Results of Metallographic Examination 40

TABLE 18
Results of Metallographic Examination 41

LIST OF FIGURES

	Page
FIGURE 1 Schematic Drawing of Hastelloy-C Autoclave	42
FIGURE 2 Teflon Coupon Racks Used to Mount Seamless and ERW Coupons	43
FIGURE 3 General Appearance of Seamless S0095 Steel Coupons Provided by Algoma Steel	44
FIGURE 4 General Appearance of Seamless L80 Steel Coupons Provided by Algoma Steel	45
FIGURE 5 General Appearance of Seamless K55 Steel Coupons Provided by Algoma Steel	46
FIGURE 6 General Appearance of ERW K-55 Steel Coupons Provided by IPSCO	47
FIGURE 7 General Appearance of ERW J-55 Steel Coupons Provided by IPSCO	48

List of Figures continued.....

FIGURE 8
General Appearance of ERW L80 Steel Coupons
Provided by IPSCO 49

FIGURE 9
Tenancious Film Formed in the K-55 materials
after exposing to a CO_2 environment (Run 1c)
Algoma K-55) 50

FIGURE 10
Blistering in surface film after a L-80 sample was
exposed to a CO_2 environment (Run #1c) for 28 days
(Algoma L-80) 51

FIGURE 11
Polished section surfaces of the as-received and exposed
(Run #1c) test coupons (Algoma K55) 52

FIGURE 12
Etched sectional surfaces of the as-received and exposed
(Run #1c) test coupons (Algoma K55) 53

FIGURE 13
Sectioned surfaces of the as-received and exposed
(Run #1c) test coupons (Ipsco K55) 54

FIGURE 14
Etched surfaces of the as-received and exposed
(Run #1c) test coupons (IPsco K55) 55

FIGURE 15
Etched surfaces of welded region of the exposed
(Run #1c) test coupons 56

1. INTRODUCTION

The corrosion of materials under the influence of carbon dioxide is of great interest to the oil and gas industry. The growing interest in enhanced oil recovery techniques has brought with it a new series of materials problems dealing with the recovery, transport, injection and production of carbon dioxide and carbon dioxide rich fluids. A possible extension of the useful life of surface piping and downhole tubular materials, if only by 50 percent, would achieve considerable reduction in capital and operating costs. Under such conditions, the importance of assessing the parameters which control the corrosion processes of carbon dioxide on tubular goods, is manifested both by technical necessity and potential economic advantages.

One of the most common types of failure of tubular goods encountered in deep well drilling and enhanced oil recovery operations is carbon dioxide corrosion. This report describes the results of a corrosion investigation directed towards determining the corrosion rates and metallurgical effects of tubular carbon steel coupons exposed to aqueous carbon dioxide/brine environments at various conditions of temperature and pressure.

2. OBJECTIVES

The objectives of the program were to characterize and elucidate the mechanism of corrosion damage affecting the performance of both ERW and seamless tubular goods in high temperature ($100^{o}C$ - $150^{o}C$) CO_2 brine environments.

Comparison of the information obtained from this study with information available in both the public and private domain on the

selection, application and in-service performance of downhole tubular goods in enhanced oil recovery projects in the U.S.A. and Canada can then be made.

3. PROCEDURES

3.1 Autoclave System

All experiments were conducted in a 2-gallon Hastelloy C autoclave. The autoclave was equipped with gas and liquid sampling ports, a gas injection line and magnetic stirring to provide solution agitation. The autoclave was heated by a 3-zone heater that provided temperature control to $\pm$ 2^{o}C of the set point. The autoclave has maximum operating pressure and temperature limits of 5,000 psi (34.47 kpa), and 500^{o}C respectively. Figure 1 is a schematic drawing of the autoclave used in the experiments.

3.2 Experimental Procedure

For the purpose of the corrosion experiments, three (3) coupons of each steel grade were mounted on a Teflon coupon tree as illustrated in Figure 2. The chemical composition of each steel grade is listed in Table 1. Each coupon was suspended on stainless steel that was coated with Teflon tubing. This ensured that each coupon did not contact any dissimilar metal surfaces. All experiments were conducted in a brine solution prepared according to ASTM D1141. Table 2 lists the concentrations of the various brine solution components. A brine prepared according to ASTM D1141 was used for the aqueous phase as this formulation has been used by other researchers for similar corrosion studies. Thus, comparison of experimental corrosion rates with published corrosion rates could be made. Sufficient brine was used such that all coupons were covered with an

aqueous phase during the experiments such that the volume/area ratio was 10ml/cm^2. It is important to note that the brine was boiled for one half hour prior to each experiment to minimize dissolved oxygen levels. As the solution pH is basic, boiling would not alter the concentration at HCO_3^-. After boiling nitrogen gas was bubbled through the cooled brine solutions to prevent the reabsorption of oxygen.

A total of 5 autoclave experiments were conducted and the specific conditions of each experiment are summarized in Table 3.

The procedure used for each experiment was conducted in the following sequence. The coupons and oxygen free brine were placed in the autoclave. The autoclave was then sealed. Carbon dioxide in the form of dry ice was added through a sampling port on top of the autoclave.

During this step, considerable boil-off of gaseous carbon dioxide occurred. This had the advantage of flushing the gas space, above the brine solution, free of oxygen. Sufficient dry ice (approximately 2 Kg of dry ice) was added to achieve a complete single component CO_2 gas phase. After addition of the dry ice, the sample port was sealed and the heaters and magnetic stirrer were switched on.

Note that due to the size of the coupons, the magnetic stirrer was run at approximately 300 rpm. Faster stir rates resulted in the coupons contacting the thermowell.

The carbon dioxide pressure was constantly adjusted during the heat-up so that the final pressure was 2,000 psi at operating temperature. At this point 2,000 psi of oxygen free nitrogen

were added to produce a final operating pressure of 4,000 psi. Gas chromatography was used to ensure that the gas phase concentration of carbon-dioxide was 50 ± 2 volume percent. Dissolved oxygen was determined using a dissolved oxygen test Kit, (Chemetrics Inc.). and was found to be less than 1 ppm for all experiments.

At the termination of an experiment, the heaters were switched off and the autoclave was allowed to cool (~ 12 hours). The coupons were removed and stored in a desiccator until weight gain and loss measurements could be conducted. As well, X-ray diffraction analyses of the chemical film of one coupon from each experiment were performed.

3.3 Coupon Preparation

The ERW and seamless carbon steel coupons were received by Ontario Research from C & M Engineering of Calgary. The ERW material was originally provided by IPSCO (Regina, Saskatchewan) and consisted of steel grades IJW55, IKW55 and IL80. The seamless material was provided by Algoma Steel (Sault Ste. Marie, Ontario) and consisted of steel grades K55, L80 and S0095. The chemical composition of the test materials is listed in Table 1. Ontario Research received a total of 25 numbered coupons, of each steel grade, prepared by C & M Engineering. The coupons were prepared by cutting them to uniform dimensions and providing surface and edge finishes suitable for the program.

The coupons had approximate dimensions of 3.5cm X 3.5cm X 0.8cm. The IJW55 samples were derived from 5 1/2" O.D., (13.97 cm), and 0.275", (0.70 cm), wall thickness ERW casing. The

IJW55 is a medium carbon, low sulphur steel in a full body normalized condition. The IKW55 samples were derived from 7" O.D., (17.78 cm), and 0.272", (0.69 cm), wall thickness ERW casing. The IKW55 is a medium carbon, low sulphur steel microalloyed with molydenum and vanadium, and in a full body normalized condition. The IL80 samples were derived from 7" O.D., (17.78 cm), and 0.362", (0.92 cm) wall thickness ERW casing. The IL80 is a medium carbon, low sulphur steel microalloyed with vanadium and molydenum, and in quenched and tempered condition.

In the case of Algoma Steel samples, they were derived from 9.5" O.D., (24.13 cm), casing. The edges had been finished to 320 grit and a glass bead technique had been used to remove mill scale from the coupon surfaces. Figures 3 to 8 illustrate the geometry and surface features of the coupons. It is important to note that the coupons were prepared from actual pipe stock. This produced coupons with curved surfaces, surface metallurgical conditions, and weld profiles that more closely simulate field applications.

For the purpose of determining corrosion rates using weight loss measurements the coupons were degreased in acetone, weighed and dimensioned to determine surface areas. All coupons were stored in a desiccator (with drying agent) until required for a particular experiment. This eliminated potential corrosion of the carbon steel surfaces by humid air.

3.4 X-ray Diffraction Analysis

X-ray diffraction analyses were conducted using a Philips recording diffractometer to identify crystalline phases present in the corrosion products. The filmed inner surface of one coupon removed from a particular experiment was used for these

analyses. Note, the scope of the program was not sufficient enough for X-ray analysis to be conducted on all steel types exposed to each of the chemical environments. All X-ray spectra were, however, carefully examined to ensure that all chemical compounds, (i.e. metal oxides, metal hydroxides, metal carbides, and metal carbonates), were detected.

3.5 Corrosion Rates

The corrosion rates were calculated from weight loss data. The measured weight losses and the calculated corrosion rates are presented in Tables 4 to 9.

Corrosion rates were calculated from weight loss data using the following equation:

$$\text{Corrosion rate } \frac{\text{mm}}{\text{yr}} = \frac{87.6\ W}{DAt}$$

87.6	=	constant to provide corrosion rates in mm/yr.
W	=	weight loss in milligrams
D	=	density in g/cm^3 (taken as $7.86\ g/cm^3$ for all steel grades)
A	=	coupon area in cm^2
t	=	experimental time in hours.

The chemical film on the coupons was removed by first cleaning in a mild detergent followed by short exposure (5 seconds) to a dilute (10%) hydrochloric acid solution. The acid cleaning was continued until most of the film had been removed. This was determined by examining the coupon surface with an optical microscope and

continuing the cleaning process until all the coupon surface was judged to be free of corrosion products.

During this process the coupon was weighed after each acid cleaning. The coupon was considered defilmed when weight losses became constant (i.e. further acid cleaning was not necessary as the coupon was now defilmed) and visual examination of the coupon surface with an optical microscope revealed that most of the crystalline film had been removed.

3.6 Variation in the Corrosion Rates of Coupons of the Same Steel Grade Exposed to a Chemical Environment.

The corrosion rate data reported in Tables 4 to 9 indicates some variation in the corrosion rates of coupons, of the same steel grade, exposed to identical environments. As well Table 10 provides a summary of the average corrosion rates and 90% confidence limits (t - distribution), for the various steels exposed to different chemical environments.This observed variation is due in part to the following:-

i) the curved geometry of the coupons made it difficult to measure coupon length and width. As a result, it is estimated that the relative error in the coupon areas is ±10%. This is based on an absolute error of ± 1mm in the length and width dimensions of each coupon;

ii) the surface finish of the coupons was variable. Although glass bead abrasion was used to remove mill scale etc., it was noted that the flat surfaces of the coupons had an irregular

non-smooth topography. The extent of the irregularity in surface finish was not consistent even among coupons of the same steel grade. In particular, coupons with very rough surfaces would be expected to have increased corrosion rates in comparison to coupons with smoother surfaces. This also introduces an error in the surface area measurement. It is difficult to estimate the magnitude of this error on the corrosion rates;

iii) the welds of the ERW materials were not uniform and there were weld trim areas which were raised slightly above adjacent base metal areas on the coupons. Variations in coupon surface areas due to the welds are also difficult to determine;

(iv) the corrosion rate data reported in Tables 4 to 9 indicated a variation in the corrosion rates among coupons of the identical steel grades exposed to the same chemical environment. This is attributed to the presence of a concentration gradient of dissolved carbon dioxide along the length of the autoclave. This gradient was produced by insufficient stirring of the brine. It is estimated that a stirring rate of at least 1,000 rpm would be required to ensure that the concentration of dissolved CO_2 in the liquid phase was not depth dependent. As previously discussed, high stir rates were not possible as this resulted in contact of the metal coupons with each other and the thermowell. As the

concentration of dissovled CO_2 is greatest near the gas/liquid phase boundary coupons mounted close to this boundary would exhibit high corrosion rates. This is precisely what is observed for experiment numbers 3, 4 and 5. Note, for experiment number 2, no CO_2 was added and the variation in corrosion rates is much less significant. Figures 1 to 4 of Appendix A, indicate the mounting configuration and clearly demonstrate the correlation of corrosion rate with mounting configuration.

3.7 Metallography

Six different types of steels were investigated in this CO_2 corrosion study. The different grades of steels were K55, L80 and S0095 from Algoma Steel Company and K55, J55 and L80 from IPSCO Steel Company. The materials provided by IPSCO contained an ERW weld in the centre of each coupon. The chemical compositions of the above materials are listed in Table 1.

Among the Algoma Steels, the K55 has a pearlitic microstructure, while the L80 and S0095 are low alloy steels with quenched and tempered martensitic microstructure. In the case of IPSCO materials, both the IJW55 and IKW-55 have fine pearlitic microstructure; whereas the ILW-80 shows quenched and tempered martensitic microstructure.

Due to the method of manufacturing, the Algoma Steel samples show a notably rougher surface even after the surface preparation treatment. Attempts at modifying the surface with acid pickling were unsuccessful. Consequently, a longer glass beading treatment was applied to the Algoma samples.

Metallographic examinations were performed on all test coupons subjected to the corrosive environments as listed in Table 3. The

exposed coupons were initially examined for general surface features, followed by a detailed metallographic examination on the cross-section of the coupons, in both polished and etched conditions.

In general, an adherent surface film was found on all samples exposed to the CO_2 test environments. This film is shown in Figure 9 on a test coupon after the first series of test runs, was found to consist of siderite, ($FeCO_3$). A very minor amount of iron was also detected on the surface of the sample. This iron content, however, is believed to be derived from the substrate.

The general observations made on the test coupons that were subjected to the different test environments are listed in Tables 13 - 18.

4. RESULTS AND DISCUSSION

4.1 Corrosion Rate Data for Coupons Exposed to a 150^0C, 50% CO_2, 4,000 psi/Brine Solution, Test Run #1 and #3

Experiments numbered 1 and 3 consisted of exposing the test coupons to a 150^0C brine solution with a gas phase carbon dioxide pressure of 2,000 psi for a period of 28-days. During experiment number 1, one coupon of each material was removed at 9, 19 and 28 day intervals. The 28 day corrosion rates for all materials were less than 0.5 mm/yr. There were no observed significant differences in the corrosion rates of the various materials. The observed decrease in corrosion rate with time, for experiment 1, indicates that the coupon surfaces are covered by a protective film early in the experiment. This passivation process is probably complete within the first nine days of the experiment. The corrosion rates are

indicative of the formation of a hard, crystalline non-permeable film with virtually no solubility in the brine solution. X-ray diffraction analysis of a coupon (S-10) exposed to the 150°C CO_2/brine environment demonstrated that the film was composed of siderite, $FeCO_3$.

4.2 Corrosion Rate Data for Coupons Exposed to a 100°C, 50% CO_2, 4000 psi/Brine Solution, Test Run #4

Experiment 4 consisted of exposing the test coupons to a 100°C brine solution with a gas phase carbon dioxide pressure of 2,000 psi for a period of 28 days. The corrosion rates for all steel grades are found in Tables 4 to 9. Except for the rates of coupons K-10 and K-11, all materials had observed corrosion rates of less than 0.1 mm/yr. It is noteworthy that the K-55 material had higher corrosion rates at 100°C than at 150°C (refer to Table 10). X-ray diffraction analysis of the filmed surface of coupon S-13 determined that siderite $FeCO_3$ was the major constituent of the film. Unidentifiable constituents comprised less than 5% of the film. Please note that a detailed examination of the X-ray data did not allow for the assignment of these constituants to an inorganic salt, ferritic phase or metal carbide.

4.3 Corrosion Rate Data For Coupons Exposed to a 150°C Brine Solution, (Total Pressure 4,000 psi N_2), Test Run #2

Experiment number 2 involved exposing the test coupons to a 150°C brine solution, to which no carbon dioxide gas had been added, for a period of 28 days. The gas phase consisted of oxygen free nitrogen with a total pressure of 4,000 psi at 150°C. The corrosion rate

data are found in Tables 4 to 9 for the different steel grades. In general the corrosion rates for all steel grades were found to be between 0.1 and 0.5 mm/yr. X-ray diffraction analysis of the chemical film indicated that the film consisted of 70% siderite, $FeCO_3$ and 30% magnetite, Fe_3O_4.

4.4 Corrosion Rate Data for Coupons Exposed to 150°C, 50% CO_2, 4000 psi/Brine Solution, Test Run #5 (Note $NaHCO_3$ and $CaCl_2$ components of the Brine were replaced with NaCl).

Experiment number 5 consisted of exposing the coupons to a 150°C, 50% CO_2, 4,000 psi environment in which $NaHCO_3$ and $CaCl_2$ had been omitted. It is important to note that an equivalent mass of NaCl was used to replace these species. All other brine components remained as outlined in Table 1. The recent literature had indicated that $NaHCO_3$ and $CaCl_2$ can contribute to the inhibition of the corrosion of carbon steel grades in aqueous carbon dioxide solutions[1]. Thus, the purpose of this experiment was to determine the significance of the role of HCO_3^- and Ca^{+2} ion in inhibiting corrosion of carbon steels in CO_2/brine solutions. The data of Tables 4 to 11 shows a magnitude increase of 2 - 3 times in the corrosion rates (compare the rates of experiments numbered 1 and 3 with experiment 5) of coupons recovered from the HCO_3^- and Ca^{+2} free brines.

4.5 Discussion of Corrosion Rate Data

The corrosion rate data generated by experiments 1 to 4 for the various steel grades indicates the following:

i) passivation of the steel surfaces occurs early, (within 9 days), during the 28-day experimental period;

ii) except for the ILW material (see Table 10) all steel grades exposed to a CO_2 free environment, experiment number 2, (i.e. no CO_2 gas added) had higher corrosion rates than identical materials exposed to the environment of experiment number 3, (50% CO_2 in the gas phase). This behaviour cannot be explained based on the results of this program. A more detailed study that related chemical and physical properties of this steel grade to the data generated from an experimental program of greater scope would be required;

(iii) the average corrosion rates of the material exposed to the 100°C CO_2/brine environment are less than those of identical materials exposed to the 150°C/brine environment. The K-55 material is a noted exception;

(iv) the data of Table 10 suggests that HCO_3^- and/or Ca^{+2} ions may inhibit corrosion of carbon steel. Compare the average corrosion rates of experiments 3 and 5. It is noted that the inhibition effect does not appear to apply to the ILW material.

The corrosion rate data accumulated from the various experiments can be partially explained with reference to the equilibrium date for CO_2 solutions. Equilibria data as a function of temperature for aqueous carbon dioxide are listed below. In particular, the following equilibria are considered.

	Keq. (100°)	Keq. (150°C)
CO_2 gas $\rightleftharpoons$ CO_2 aqueous	1.01×10^{-2}	8.24×10^{-3}
CO_2 aqueous + $H_2O \rightleftharpoons H^+ + HCO_3^-$	3.69×10^{-7}	1.8×10^{-7}
$HCO_3^- \rightleftharpoons H^+ + CO_3^{2-}$	7.06×10^{-11}	4.43×10^{-11}

The ratio of the equilibrium constants for the solubility of carbon dioxide in water at 100°C and 150°C is 1.2:1

$$\frac{[CO_2](100^oC)}{Pco_2(100^oC)} = 1.2 \times \frac{[CO_2](150^oC)}{Pco_2(150^oC)}$$

NOTE:

Pco_2 (100°C) = Pco_2 (150°C) = 2,000 psi

$\therefore$ $[CO_2]100^oC \cong 1.2\ [CO_2]\ 150^oC$.

$[CO_2]$ = concentration of CO_2 in aqueous phase in moles/litre

Thus the solubilities of carbon dioxide in 100°C and 150°C aqueous solutions are similar. In addition, there is little difference between the equilibrium constants for the formation of HCO_3^- and CO_3^{2-} anions. This implies that a temperature increase from 100°C to 150°C has very little influence on changes in the equilibria of CO_2, HCO_3^- and CO_3^{2-} in aqueous solution. Thus, it is not surprising the corrosion rates, calculated from 28-day experiments conducted at 100°C and 150°C are similar. It should be noted that the rates of the CO_2 corrosion at 150°C should be greater than at 100°C. However, passivation at both temperatures is probably complete within a few days. Therefore, differences in the corrosion rates due to temperature dependent

kinetic effects would not be detected in data collected from 28-day experiments.

The exposure of the coupons to an environment in which CO_2 gas was not added produced corrosion rates that were greater, in magnitude, than those produced by exposure to a carbon dioxide/brine solution. In addition, the films of these coupons consisted of approximately 70 percent siderite and 30 percent magnetite. This indicates that coupons are corroding by two possible mechanisms. Magnetite can form via the Schikorr reaction:

$$3\ Fe + 4H_2O \rightleftharpoons Fe_3O_4 + H_2$$

Siderite is produced by the direct reaction of the coupon steel with carbonic acid or by the interaction of Fe^{+2} with HCO_3^- or CO_3^{2-}. The main source of carbonate and bicarbonate ions was the sodium bicarbonate salt used to prepare the brine.

$$Fe^{+2} + HCO_3^- \rightleftharpoons FeCO_3 + H^+$$

(Fe^{+2} is produced by some other corrosion mechanism i.e. the Schikorr reaction).

$$Fe + H_2CO_3 \rightleftharpoons Fe\ CO_3 + H_2$$

The carbonic acid is produced by the hydrolysis of the sodium bicarbonate component of the brine solution:

$$NaHCO_3 + H_2O \rightleftharpoons H_2\ CO_3 + NaOH$$

This experiment indicates that bicarbonate ion, introduced as

$NaHCO_3$, in the brine, actively participates in the corrosion of the steel coupons. It is noteworthy that this species is in competition with water which also oxidizes the metal surface. It is reasonable to conclude that large pressures of carbon dioxide gas therefore provide enhanced levels of HCO_3^- anion and thus suppress the Schikorr reaction. The slightly enhanced corrosion rates of the coupons recovered from experiment number 2 are attributed to the participation of the Schikorr reaction in the overall corrosion scenario.

There is some speculation in the literature [1,2,3] that the presence Ca^{+2} and HCO_3^- ions in brine solutions suppresses corrosion of steel surfaces. To determine the importance of these ions with respect to the corrosion rates an experiment was conducted in which both Ca^{+2} and HCO_3^- were replaced with equivalent weights of sodium chloride. The results are reported for experiment number 5 in Tables 3 to 9.

Comparison of the average corrosion rates (Table 10) for experiment numbers 3 and 5 suggests that the absence at HCO_3^- and Ca^{+2} increase the corrosion rates by a factor of 2-3 except in the case of the ILW-80 material.

4.6 Results of Metallographic Examination Test Run #1

4.6.1 Test Run #1

For the purpose of this discussion, Runs #'s 1a, 1b, and 1c refer to the 9, 19 and 28 day intervals of Experiment 1. A surface film, consisting mainly of siderite, was formed when a sample (derived from K55, L80, or S0095) was exposed to the CO_2 environment (#1a) for

only 9 days.Figure 9 shows the film on a K55 steel which was formed after exposing the coupon to a CO_2 environment (Run #1c), for 28 days.

On examining the exposed surfaces of the above samples, it was found that the surface films formed on the K55 and L80 steels were less tenacious than those formed an S0095. In addition, the surface films formed in the former steels tended to blister when exposed for a longer time in the same CO_2 environment.

This blistering phenomenon is evident in the L80 sample (Figure 10) after exposure to a CO_2 environment (Run #1c). Apparently, blistering resulted from rupturing of the outer layers of the surface film. The inner layers, however, were still intact with the metal surface.

On examining the microstructure of the substrate, no identifiable localized corrosion was found in K55, L80 or S0095 steels after the first series of test runs (1a,1b and 1c). Even in the K55 steel, which is the lowest alloy grade among the three materials, the coupons did not corrode in the CO_2 environment (Run #1). Figures 11 and 12 show the sectioned surfaces of the as-received and exposed (Run #1c) K55 test coupons, in both polished and etched conditions respectively. No noticeable form of corrosion can be resolved with the optical microscope on the exposed samples.

Quite similar to the Algoma Steels, the IPSCO steels were not subjected to any visible form of corrosion other than uniform corrosion after being exposed to the CO_2 environments (Runs 1a,1b and 1c). Figures 13 and 14 show the sectioned surfaces of IKW 55 steels in both polished and etched conditions respectively. No visible form of corrosion attack other than uniform corrosion was found in this material after the completion of test run #1. Welded

regions of the test materials were also examined for corrosion damage and no selective damage was found in the HAZ. Figure 15 shows the area in the welded region, which does not show any visible form of corrosion other than uniform corrosion (Run 1 a, b and c). Other grades of steels, such as J55 and L80 steels, had exhibited similar corrosion resistant properties.

4.6.2 Test Run #2

The objective in performing this test run was to assess, if the CO_2 environment was promoting the formation of a tenacious film. It is believed that this film acted as a protective surface, which inhibits any form of corrosion attack. On examining the test coupons (IPSCO - IKW55, IJW55 and ILW80; Algoma K55, L80 and S0095) which were exposed to the test environment in Run#2, no notable form of corrosion other than uniform corrosion was detected.

Despite the fact that CO_2 gas was not added to the test environment, the analysis of the surface film by X-ray diffractometry showed that the major constituents of the deposit were siderite ($FeCO_3$) and magnetite (Fe_3O_4) in the approximate ratio of siderite 70%: magnetite 30%.

4.6.3 Test Run #3

The test environment in Run#3 was actually identical to Run#1. In the case of Run#3, samples were exposed to the test condition for 28 days continuously. In the case of Run#1c, samples were subjected to two brief temperature cycles, when samples were retrieved from the autoclave. Regardless of the minor difference in the experimental condition, the results of the metallographic examination on the test coupons are identical. No visible form of corrosion attack other

than uniform corrosion was found in the test coupons.

4.6.4 Test Run #4

In this test run, a test temperature of 100°C was selected. It has been reported that the CO_2 corrosion attack on steels is most severe at this temperature. Despite the previous claim, no corrosion attack other than uniform corrosion was observed on the test samples exposed to the above environment. The formation of the tenacious film, apparently, had provided a very protective coating, which inhibited the corrosion attack.

4.6.5 Test Run #5

In view of the findings in the previous runs, that the film on the coupons exposed to both the CO_2 and CO_2 free environments was composed mainly of siderite, the data indicate that the HCO_3^- anion component of the brine was actively participating in the formation of the protective film. In addition, it has been found that Ca^{2+} [1] also contributes in inhibiting the corrosion of steels. Consequently, in test Run#5, coupons were exposed to an HCO_3^- and Ca^{2+} free environment.

Despite the above changes in the environmental condition, no visible corrosion attack other than uniform corrosion was found on the test coupons.

5. SUMMARY AND CONCLUSIONS

This study has demonstrated that in the 100°C - 150°C temperature range the corrosion of both seamless and ERW carbon steels exposed to 2,000 psi partial pressures of CO_2 and brine is less than 0.5 mm/yr.

The corrosion product is siderite, $FeCO_3$. The siderite is produced in the form of a very hard crystalline film that passivates the metal surface. Preliminary data is provided to indicate that HCO_3^- and possibly Ca^{+2} ions do potentially inhibit corrosion. In addition, HCO_3^- ion, introduced as $NaHCO_3$ in the brine of CO_2 free solutions also contributes to the corrosion of steel surfaces. This was verified in experiment number 2 by the detection of $FeCO_3$, along with Fe_3O_4, in the corrosion products.

These low corrosion rates are consistent with those reported in the literature for similar experiments. In particular, tests performed on a J-55 steel coupon exposed to an O_2 free aqueous solution with a partial pressure of 13 bars, (187 psi) at 54°C resulted in a corrosion rate of 0.35 mm/yr after 28 days[2].

Other tests conducted at 163°C with CO_2 partial pressures of 1500 psi in a brine composed of NaCl produced corrosion rates on carbon steels of approximately 1.5 mm/yr. (Time of experiment less than 200 hours)[4]. Indeed, temperatures of 100°C and 150°C were demonstrated to produce low corrosion rates. The results reported in this study indicated the following:-

i) the surfaces of carbon steel coupons are passivated with time to produce corrosion rates of less than 2 mm/yr, (168 hour experiment);

ii) increases in CO_2 partial pressure produced a decrease in the corrosion rate of carbon steels. For experiments conducted at 150°C in a brine an increase in partial CO_2 pressure from 100 to 300 psi decreased corrosion rates from 0.736 mm/yr to 0.381 mm/yr. (less than 200 hr. exposure);

iii) the longer the experimental time period the lower the corrosion rates;

iv) due to the low solubility of $FeCO_3$ at high temperatures corrosion rates decrease with temperature.

The corrosion data reported for experiment numbers 1 to 5 are consistent with data reported in the literature for similar experiments. To ensure that the autoclave system was not artificially lowering the corrosion rates of the coupons, four coupons K-17, K-18, IJW-1 and IJW-8 were exposed to 150°C/brine solution with a partial pressures of 100 psi O_2 and 3900 psi nitrogen for a period of 7 days. These coupons had corrosion rates of 13.69, 12.75, 16.02 and 13.58 mm/yr., respectively. These corrosion rates demonstrate that the autoclave system was not contributing to the inhibition of corrosion of carbon steels by aqueous carbon dioxide/brine solutions. As well, the presence of dissolved oxygen in the brine yields an environment that is corrosive to carbon steel.

6. COMPARISON OF CORROSION RATES FROM LABORATORY AND FIELD STUDIES

In general corrosion rates from field studies are greater than those measured in the laboratory. This is due to the increased complexity of real as opposed to artificial brines. Real brines may contain organic acids capable of participating in the overall corrosion process. In addition, flow rates in oil well and gas tubing are much higher, (the order of metres/second), as compared to the flow rates generated in a stirred autoclave. As well, flow cycling of the wells introduces stresses and thermal cycling, which are not considered in laboratory experiments. The data reported for this experimental study do not account for the influence of thermal and flow cycling on corrosion rates.

The corrosion rate data collected for the steel grades provided for the program, are less than 0.5 mm/yr. Thus, these materials have good corrosion resistance, (see Table 12), to 100°C - 150°C CO_2/brines. This suggests that these materials may be suitable for use in steam stimulation projects in which downhole temperatures of 150°C and higher are not uncommon. However, it is not clear as to whether the materials are suitable for CO_2 flood methods. Carbon dioxide flooding is not a thermal recovery method and well tubular products are exposed to temperatures below 100°C. Corrosion rate data in this temperature range would be required to assess the utility of these materials for use in CO_2 flooding projects.

7. FUTURE STUDIES

The experiments conducted in this program do indicate that calcium chloride and sodium bicarbonate inhibit corrosion of carbon steels by CO_2/brine soltions in the 100°C - 150°C temperature range. Thus, it would be useful to determine if this inhibtion effect also operates in the presence of hydrogen sulphide. A series of comparative experiments should be conducted in which the corrosion rates of carbon steels in the presence of CO_2/H_2S brines that contain both HCO_3^- and Ca^{+2} ions are determined. These results should be compared to the results of identical experiments conducted in HCO_3^- and Ca^{+2} free brines. This would establish the ability of HCO_3^- and Ca^{+2} ion to inhibit corrosion in H_2S/CO_2 brines.

J. D. Tyrer, Ph.D.
Scientist
Materials Division

S. H. Lo, Ph.D.
Scientist
Materials Division

R. T. Lassau, Head
Materials Corrosion/Metals Investigations

BIBLIOGRAPHY

1. Burke, P.A., "Synopsis: Recent Progress in the Understanding of CO_2 Corrosion" Advances in CO_2 Corrosion Vol. 1: Proceedings of the Corrosion/83 Symposium in CO_2 Corrosion in the Oil and Gas Industry. pp.3.

2. Schmitt, G.,"Fundamental Aspects pf CO_2 Corrosion", Ibid., pp 10-19.

3. Eriksrud, E & Sontvedt, T."Effect of Flow on CO_2 Corrosion Rates in Real and Synthetic Formation Waters, Ibid., pp. 20-38.

4. Hausler, R.H."The Mechanism of CO_2 Corrosion of Steel in Hot, Deep Gas Wells, Ibid., pp. 72-86.

TABLE 1

Chemical Compositions of Test Materials

		C	Mn	P	S	Si	Cr	Mo	Al
Algoma	K55	0.47	1.01	0.018	0.015	0.30	0.05	0.02	0.046
	L80	0.27	1.36	0.023	0.017	0.31	0.10	0.06	0.046
	S0095	0.29	1.30	0.023	0.016	0.31	0.09	0.06	0.037
IPSCO	IJW-55	0.25	1.38	0.011	0.005	0.25	--	--	0.027
	IKW-55	0.288	0.96	0.010	0.002	0.26	--	0.159	0.007
	ILW-80	0.265	0.92	0.012	0.003	0.25	--	0.166	0.052

TABLE 2

BRINE COMPOSITION
(ASTM - D1141)

The brine solution was prepared by combining 245.34g of NaCl and 40.94g of anhydrous Na_2SO_4 in 8L of water.. A 200 mL aliquot and 100 mL a aliquot of stock solutions No. 1 and No. 2 were added to this solution. The total solution volume was diluted to 10.0L and the pH adjusted to 8.2 with 0.1 N NaOH.

Stock Solution No. 1

$MgCl_2$ 6 H_2O	556.6 g/L
$CaCl_2$ (anhydrous)	57.9 g/L
$SrCl_2$ $6H_2O$	2.1 g/L

Stock Solution No. 2

KCl	69.5 g/L
$NaHCO_3$	20.1 g/L
KBr	10.1 g/L
H_3BO_3	2.7 g/L
Na F	0.3 g/L

TABLE 3

Autoclave Experiment Test Run#	Experimental Conditions
1	50% CO_2, 50% N_2 150°C, 4,000 psi, coupons removed at 9, 19 and 28 days.
2	0% CO_2, 100% N_2 150°C, 4,000 psi, 28 days.
3	50% CO_2, 50% N_2 150°C, 4,000 psi, 28 days.
4	50% CO_2, 50% N_2 100°C, 4,000 psi, 28 days.
5	50% CO_2, 50% N_2 150°C, 4,000 psi, 28 days Note: brine $NaHCO_3$ and $CaCl_2$ free.

TABLE 4

CORROSION RATE DATA FOR

K-55 SEAMLESS SPECIMENS

Coupon No.	Experiment No.	Weight Gain (mg)	Weight Loss (mg)	Corrosion Rate mm/yr
K- 1	1	75.1	117.3	0.1366
K- 2	1	98.5	146.1	0.0771
K- 3	1	25.6	95.3	0.0356
K- 4	2	92.9	572.8	0.2116
K- 5	2	29.6	451.2	0.1666
K- 6	2	5.4	435.6	0.1702
K- 7	3	157.2	200.8	0.0802
K- 8	3	737.5	100.9	0.0360
K- 9	3	35.2	78.5	0.0321
K-10	4	458.6	480.2	0.1778
K-11	4	17.7	46.6	0.0198
K-12	4	63.9	660.1	0.2328
K-13	5	103.1	407.6	0.1491
K-14	5	31.1	332.6	0.1282
K-15	5	27.4	313.9	0.1266

TABLE 5

CORROSION RATE DATA FOR
L-80 SEAMLESS SPECIMENS

Coupon No.	Experiment No.	Weight Gain (mg)	Weight Loss (mg)	Corrosion Rate mm/yr
L-1	1	78.2	113.5	0.1364
L-2	1	59.2	167.7	0.0933
L-3	1	2.6	110.6	0.0409
L- 4	2	106.5	562.9	0.2104
L- 5	2	48.7	576.7	0.1939
L- 6	2	3.7	415.9	0.1643
L- 7	3	102.5	242.5	0.0946
L- 8	3	933.7	105.2	0.0390
L- 9	3	84.5	117.2	0.0470
L-10	4	55.3	78.0	0.0306
L-11	4	61.0	83.3	0.0321
L-12	4	25.0	53.5	0.0215
L-14	5	259.5	890.8	0.3315
L-15	5	66.1	427.5	0.1550
L-16	5	85.8	445.4	0.1731

TABLE 6

CORROSION RATE DATA FOR
S0095 SEAMLESS SPECIMENS

Coupon No.	Experiment No.	Weight Gain (mg)	Weight Loss (mg)	Corrosion Rate mm/yr
S-1	1	64.96	101.0	0.1460
S-2	1	8.7	92.4	0.0566
S-3	1	149.2	204.6	0.0895
S- 4	2	78.8	994.1	0.4263
S- 5	2	16.6	948.8	0.3818
S- 7 *				
S- 8	3	251.5	281.7	0.1048
S- 9	3	154.5	196.1	0.0660
S-10	3	311.9	110.1	0.0391
S-11	4	45.7	68.1	0.0235
S-12	4	57.2	86.3	0.0293
S-13	4	43.8	70.0	0.0226
S-14	5	158.6	554.0	0.1887
S-15	5	16.2	340.9	0.1264
S-16	5	7.7	364.8	0.1286

*This coupon was damaged and could not be used to determine a corrosion rate.

TABLE 7

CORROSION RATE DATA FOR
IJW-55 ERW SPECIMENS

Coupon No.	Experiment No.	Weight Gain (mg)	Weight Loss (mg)	Corrosion Rate mm/yr
IJW-1	1	63.5	112.2	0.1836
IJW-2	1	35.1	108.8	0.0744
1JW-3	1	28.0	55.4	0.0260
IJW- 4	2	96.5	464.5	0.2003
IJW- 5	2	4.5	325.2	0.1477
IJW- 6	2	22.1	375.2	0.1458
IJW- 7	3	186.9	398.0	0.1683
IJW- 8	3	74.51	105.3	0.0502
IJW- 9	3	66.7	95.9	0.0452
IJW-10	4	60.9	102.0	0.0478
IJW-11	4	82.7	103.3	0.0467
IJW-12	4	67.5	83.3	0.0377
IJW-13	5	149.8	463.6	0.1879
IJW-14	5	101.0	424.8	0.1902
IJW-15	5	117.9	433.2	0.1803

TABLE 8

CORROSION RATE DATA FOR
IKW-55 ERW SPECIMENS

Coupon No.	Experiment No.	Weight Gain (mg)	Corrosion Weight Loss (mg)	Rate mm/yr
IKW-1	1	84.95	130.5	0.1800
IKW-2	1	82.39	128.2	0.0906
IKW-3	1	18.73	38.6	0.0177
IKW- 4	2	93.29	385.9	0.1711
IKW- 5	2	101.97	332.2	0.1537
IKW- 6	2	55.52	290.9	0.1321
IKW- 7	3	233.3	265.2	0.1184
IKW- 8	3	113.3	144.2	0.0633
IKW- 9	3	115.2	140.0	0.0631
IKW-10	4	92.83	112.5	0.0514
IKW-11	4	126.1	147.7	0.0709
IKW-12	4	133.8	159.4	0.0769
IKW-13	5	223.3	531.5	0.2579
IKW-14	5	52.5	318.5	0.1585
IKW-15	5	51.5	330.9	0.1535

TABLE 9

CORROSION RATE DATA FOR
ILW-80 ERW SPECIMENS

Coupon No.	Experiment No.	Weight Gain (mg)	Weight Loss (mg)	Corrosion Rate mm/yr
ILW-1	1	66.64	106.28	0.1699
ILW-2	1	45.70	107.60	0.0598
ILW-3	1	14.34	84.23	0.0394
ILW- 4	2	53.88	340.8	0.1688
ILW- 5	2	43.07	283.9	0.1434
ILW- 6	2	9.58	264.6	0.1257
ILW- 7	3	357.4	461.3	0.2198
ILW- 8	3	164.2	241.3	0.1169
ILW- 9	3	153.9	221.3	0.0972
ILW-10	4	38.75	73.38	0.0341
ILW-11	4	30.67	62.40	0.0299
ILW-12	4	33.27	64.15	0.0316
ILW-13	5	196.85	473.8	0.1111
ILW-14	5	46.89	321.5	0.0428
ILW-15	5	30.17	283.2	0.0340

TABLE 10

AVERAGE CORROSION RATES (mm/yr) AND
90% CONFIDENCE LIMIT CALCULATOR
FROM t DISTRIBUTION

Carbon Steel	Experiment Number 2	3	4	5
K 55	0.1828 ± 0.0421	0.0494 ± 0.0438	0.2953*	0.1346 ± 0.0211
L 80	0.1895 ± 0.0392	0.0602 ± 0.0505	0.0281 ± 0.0096	0.2198 ± 0.1636
S0095	0.4041*	0.0699 ± 0.0556	0.0251 ± 0.0061	0.1479 ± 0.0595
IJW55	0.1646 ± 0.0521	0.0879 ± 0.1173	0.0441 ± 0.0084	0.1861 ± 0.0087
IKW55	0.1523 ± 0.0329	0.0816 ± 0.0537	0.0664 ± 0.0224	0.1899 ± 0.0991
ILW80	0.1459 ± 0.0365	0.1446 ± 0.1109	0.0318 ± 0.0035	0.0626 ± 0.0711
Experimental Conditions	0% CO_2 100%N_2, 150°C 4,000psi 28 days	50% CO_2 50%N_2, 150°C 4,000psi 28 days	50%CO_2, 50%N_2 100°C, 4000psi, 28 days	50%CO_2, 50%N_2, 150°C, 4,000psi 28 days Note: Brine $NaHCO_3$ and $CaCl_2$ free

*Note: only two measurements available, therefore t - test not applicable. Also data from experiment 1 was collected from three time intervals, thus statistical analysis are not appropriate. Note corrosion rate data for coupon K-11, experiment number 4, was not consistent with corrosion rate data for coupons K-10 and K-12. Thus this measurement was not used to calculate the average corrosion rate and the t - test could not be applied to this set of data.

TABLE 11

RATIO OF THE AVERAGE CORROSION
RATES FOR EXPERIMENT NUMBERS 3 and 5

Carbon Steel Type	Ratio of Average Corrosion Rate (Experiment Number 5/ Experiment Number 3)
K55	2.7
L80	3.6
S0095	2.1
IJW55	2.1
IKW55	2.3
ILW80	0.4

TABLE 12

Correlation of Corrosion Resistance and Corrosion Rate

Relative Corrosion Resistance	Corrosion Rate mm/yr
Outstanding	< 0.02
Excellent	0.02 - 0.1
Good	0.1 - 0.5
Fair	0.5 - 1
Poor	1 - 5
Unacceptable	5+

NOTE: Data from this table were produced from Fontana, M.G. and Greene, N.D. "Corrosion Engineering", McGraw Hill Book Company, New York, 1978.

TABLE 13

RESULT OF METALLOGRAPHIC EXAMINATION OF ALGOMA STEELS

Experiment Conditions / Type of Material	As Received	4000 psi 150°C 50% CO_2, 50% N_2 9 days	4000 psi 150°C 50% CO_2, 50% N_2 18 days	4000 psi 150°C 50% CO_2, 50% N_2 28 days
ALGOMA K-55	• Very Rough Surface • Surface decarburized	• Very rough surface • Surface decarburized • Presence of adherent surface film*	• Very rough surface • Few blisters on adherent surface film • Surface decarburized	• Very rough surface • Blistering on adherent surface film • Surface decarburized
ALGOMA L - 80	• Very rough surface	• Very rough surface • Formation of adherent surface film	• Very rough • some blistering on adherent film	• Very rough • Blistering on surface film
ALGOMA S00 - 95	• Rough	• Rough	• Rough	• Rough surface • No observable blistering on surface film

* Chemical composition of the surface film is presently being analyzed

TABLE 14

RUN #1

RESULT OF METALLOGRAPHIC EXAMINATION OF IPSCO STEELS

Type of Material \ Experimental Conditions	As Received	4000 psi 150°C Run 1 a 50% CO_2, 50% N_2 9 days	4000 psi 150°C Run 1 b 50% CO_2, 50% N_2 18 days	4000 psi 150°C Run 1 c 50% CO_2, 50% N_2 28 days
IPSCO K-55	Rough Surface	• Rough surface • Formation of an adherent surface film • No observable effect on HAZ	• Rough surface • Adherent surface film • Pin-hole size blistering on surface • No observable effect on HAZ	• Rough surface • Adherent surface film • Pin-hole size surface blistering • No observable effect on HAZ
IPSCO J-55	Rough Surface	• Adherent oxide film • No observable effect on HAZ	• Blistering observed on adherent surface film • No observable effect on HAZ	• Large area of blistering of adherent surface film • No observable effect on HAZ
IPSCO L - 80	Rough Surface	• Adherent oxide film • No observable effect on HAZ	• some blistering on surface film • No observable effect on HAZ	• adherent surface film • No observable effect on HAZ

TABLE 15

RUN#2 - 0% CO_2, 100% N_2, 4000 psi, 150°C for 28 days

Type of Material / Experimental Condition	2	Type of Material / Experimental Condition	2
IPSCO K - 55	• Rough Surface • Formation of an adherent surface film • smooth surface along welded region	ALGOMA K - 55	• Very rough surface • Formation of a tenacious film
IPSCO J - 55	• Rough Surface • Formation of an adherent surface film • smooth surface along welded region	ALGOMA L - 80	• Very rough surface • Formation of a tenacious film & corrosion product
IPSCO L - 80	• Rough Surface • Formation of surface film • smooth surface along welded region	ALGOMA S00-95	• Very rough surface • Formation of a tenacious film

TABLE 16

RESULTS OF METALLOGRAPHIC EXAMINATION

RUN#3 - 50% CO_2, 50% N_2, 4000 psi, 150°C for 28 days

Type of Material / Experimental Conditions	3	Type of Material / Experimental Conditions	3
IPSCO K - 55	• Rough surface • slightly decarbonized surface	ALGOMA K - 55	• severe surface decarbonization • very rough surface
IPSCO J - 55	• Rough surface	ALGOMA L - 80	• surface decarbonization • very rough surface
IPSCO L - 80	• Rough surface	ALGOMA S00-95	• rough surface

TABLE 17

RESULTS OF METALLOGRAPHIC EXAMINATION

RUN #4 - 52% CO_2, 48% N_2, 4000 psi, 100°C for 28 days.

Type of Material / Experimental Condition	4	Type of Material / Experimental Condition	4
IPSCO K - 55	• Rough surface • some decarbonization • No visible form of corrosion other than uniform corrosion	ALGOMA K - 55	• Surface decarbonized • No visible form of corrosion other than uniform corrosion
IPSCO J - 55	• Rough surface • No visible form of corrosion other than uniform corrosion	ALGOMA L - 80	• surface decarbonized • No visible form of corrosion other than uniform corrosion
IPSCO L - 80	• Rough surface • No visible form of corrosion other than uniform corrosion	ALGOMA S00-95	• surface decarbonized • No visible form of corrosion other than uniform corrosion

TABLE 18

RESULTS OF METALLOGRAPHIC EXAMINATION

RUN #5 - 50% CO_2, 50% N_2, 4000 psi, 150°C for 28 days

Type of Material / Experimental Condition	5	Type of Material / Experimental Condition	5
IPSCO K - 55	• no visible form of corrosion other than uniform corrosion	ALGOMA K - 55	• no visible form of corrosion other than uniform corrosion
IPSCO J - 55		ALGOMA L - 80	• no visible form of corrosion other than uniform corrosion
IPSCO L - 80	• no visible form of corrosion other than uniform corrosion	ALGOMA S00-95	• no visible form of corrosion other than uniform corrosion

FIGURE 1

SCHEMATIC DRAWING
OF HASTELLOY-C AUTOCLAVE

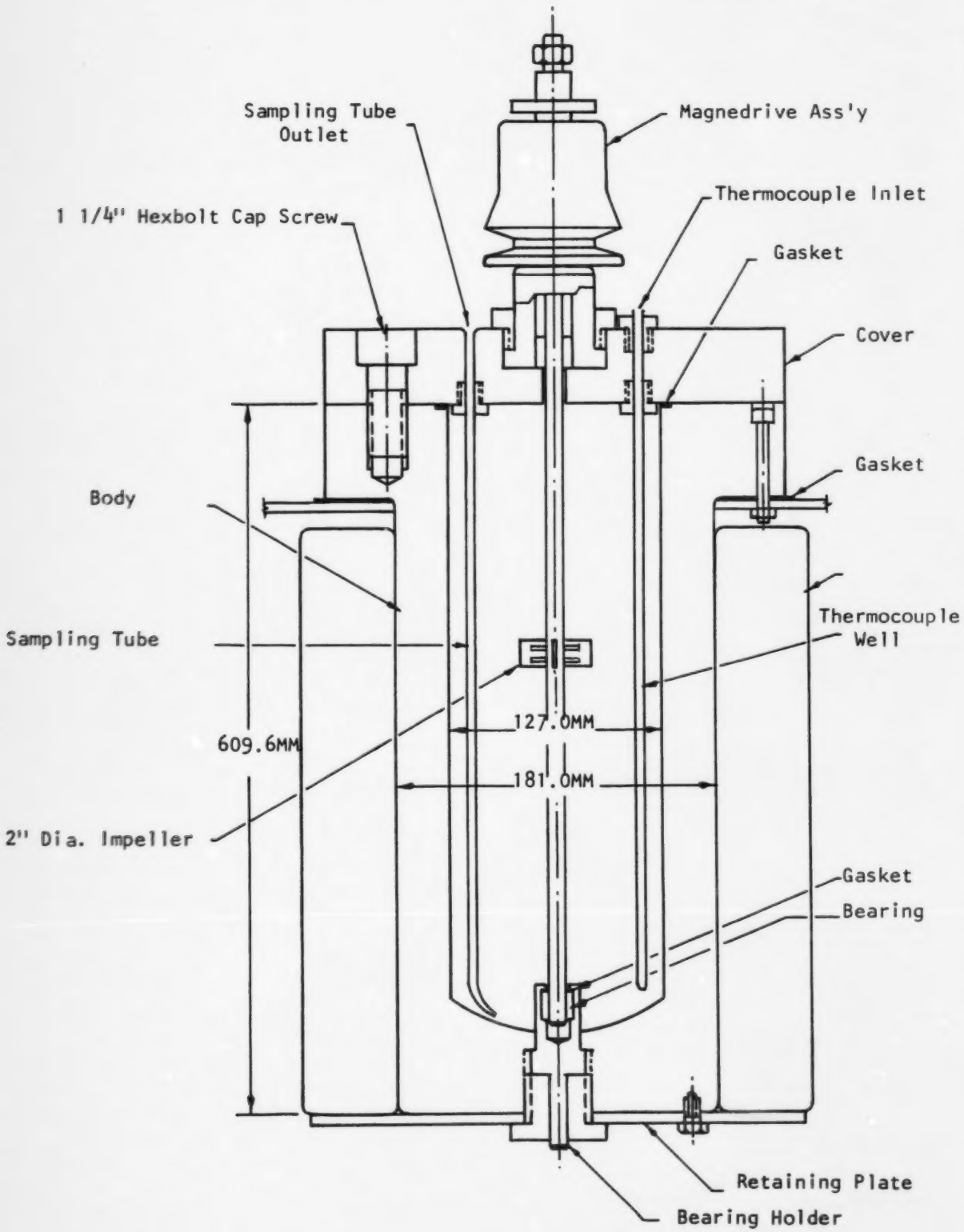

FIGURE 2

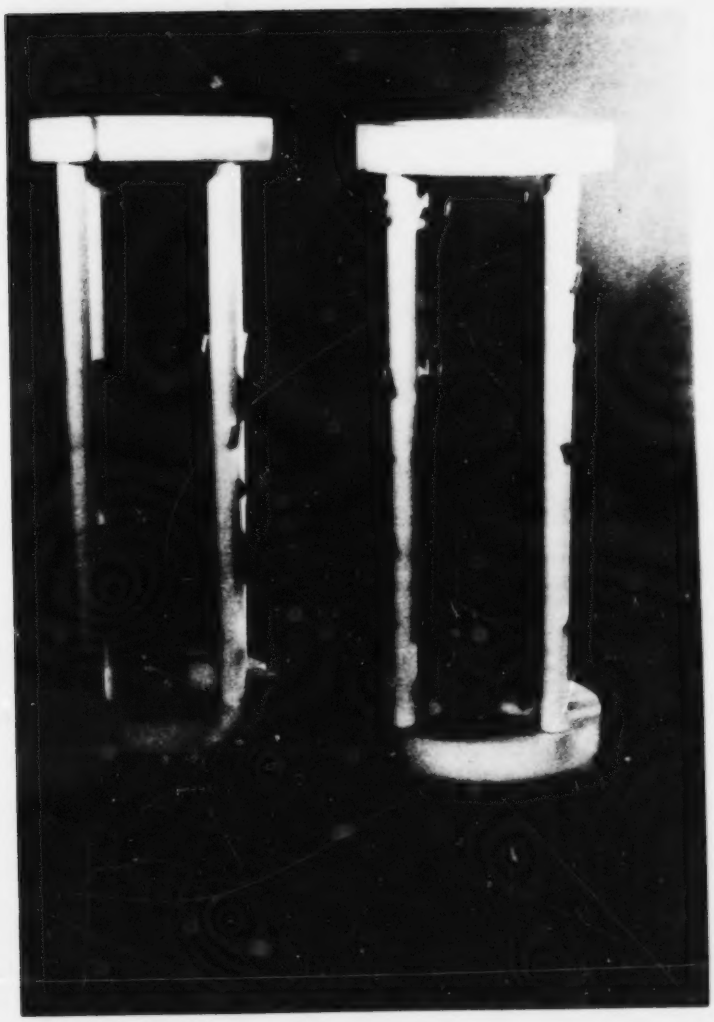

Teflon Coupon Racks
Used to Mount Seamless
and ERW Coupons

FIGURE 3

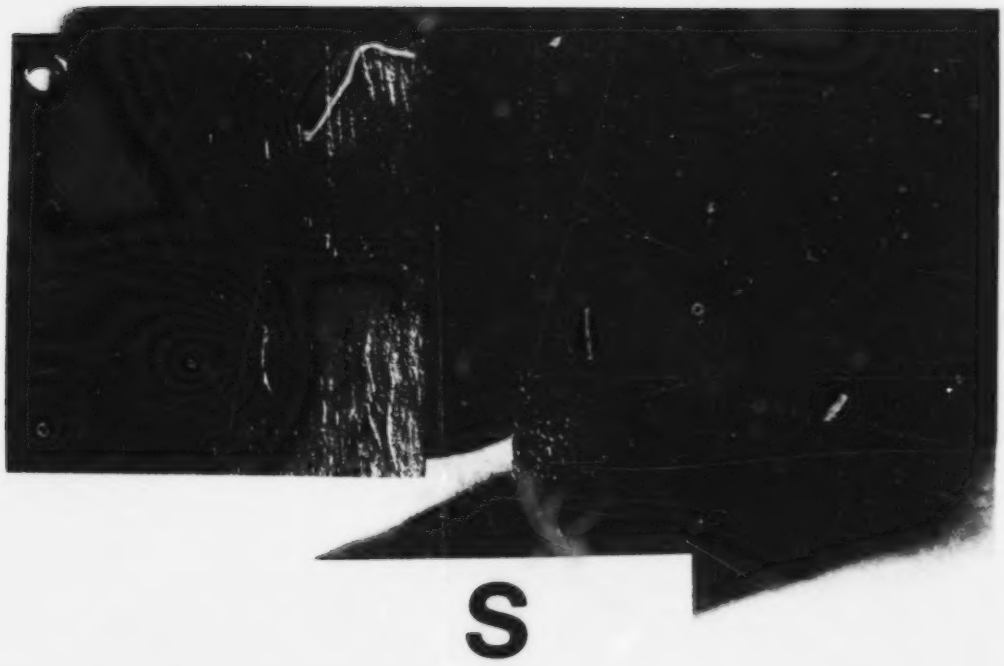

S

General Appearance of Seamless
S0095 Steel Coupons Provided By
Algoma Steel

FIGURE 4

General Appearance of Seamless L80
Steel Coupons Provided by
Algoma Steel

FIGURE 5

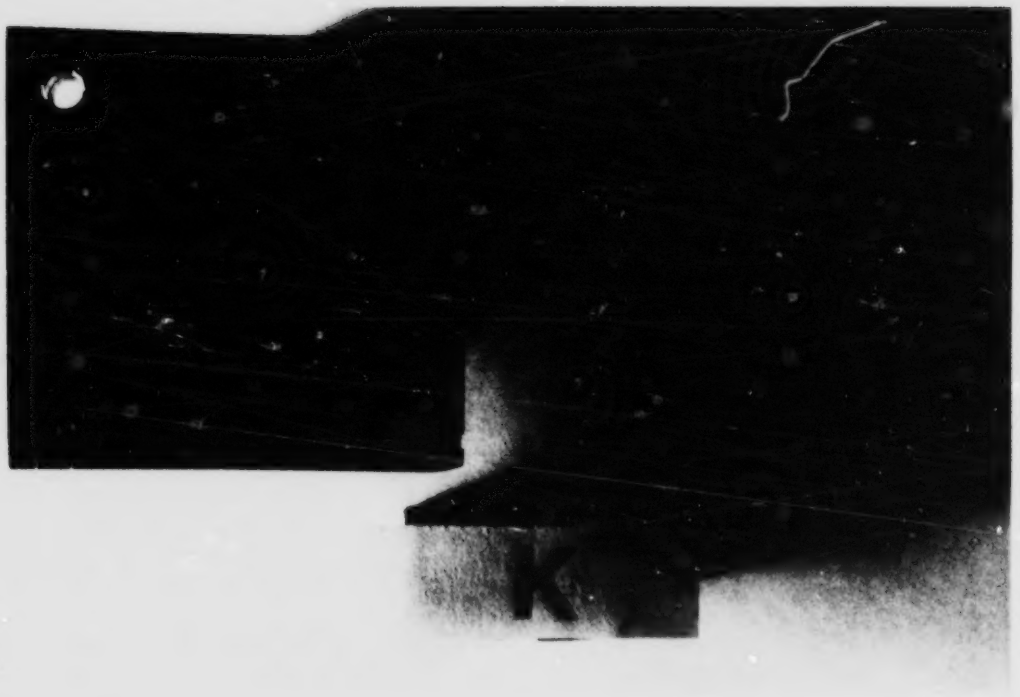

General Appearance of Seamless K55 Steel
Coupons Provided by Algoma Steel

FIGURE 6

General Appearance of ERW K-55
Steel Coupons Provided by IPSCO

FIGURE 7

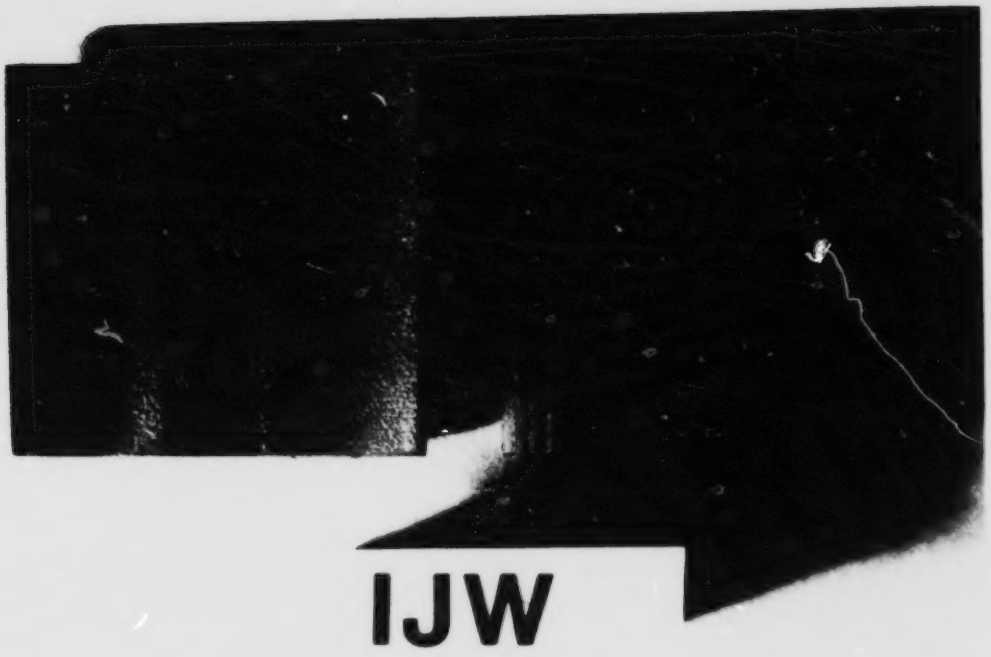

General Appearance of ERW J-55
Steel Coupons Provided by
IPSCO

FIGURE 8

General Appearance of ERW L80 Steel Coupons
Provided by IPSCO

FIGURE 9

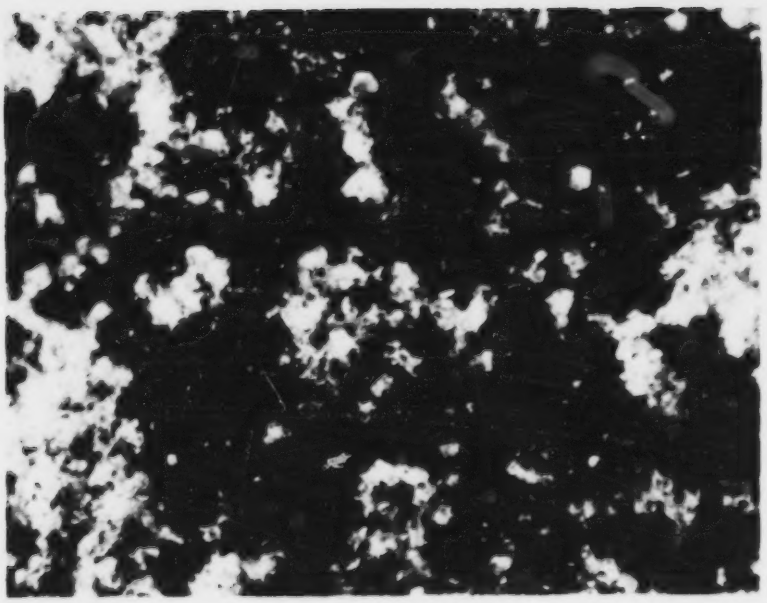

Tenancious film formed in the K-55 materials
after exposing to a CO_2 environment
(Run 1c) (Algoma K-55)

Mag. 160 X

FIGURE 10

Blistering in surface film after a L-80 sample was exposed to a CO_2 environment (Run #1c) for 28 days. (Algoma L-80)

Mag. 100 X

FIGURE 11

As-received coupon Exposed coupon

Polished section surfaces of the as-received and exposed (Run #1c) test coupons (Algoma K55)

Mag. 500 X

FIGURE 12

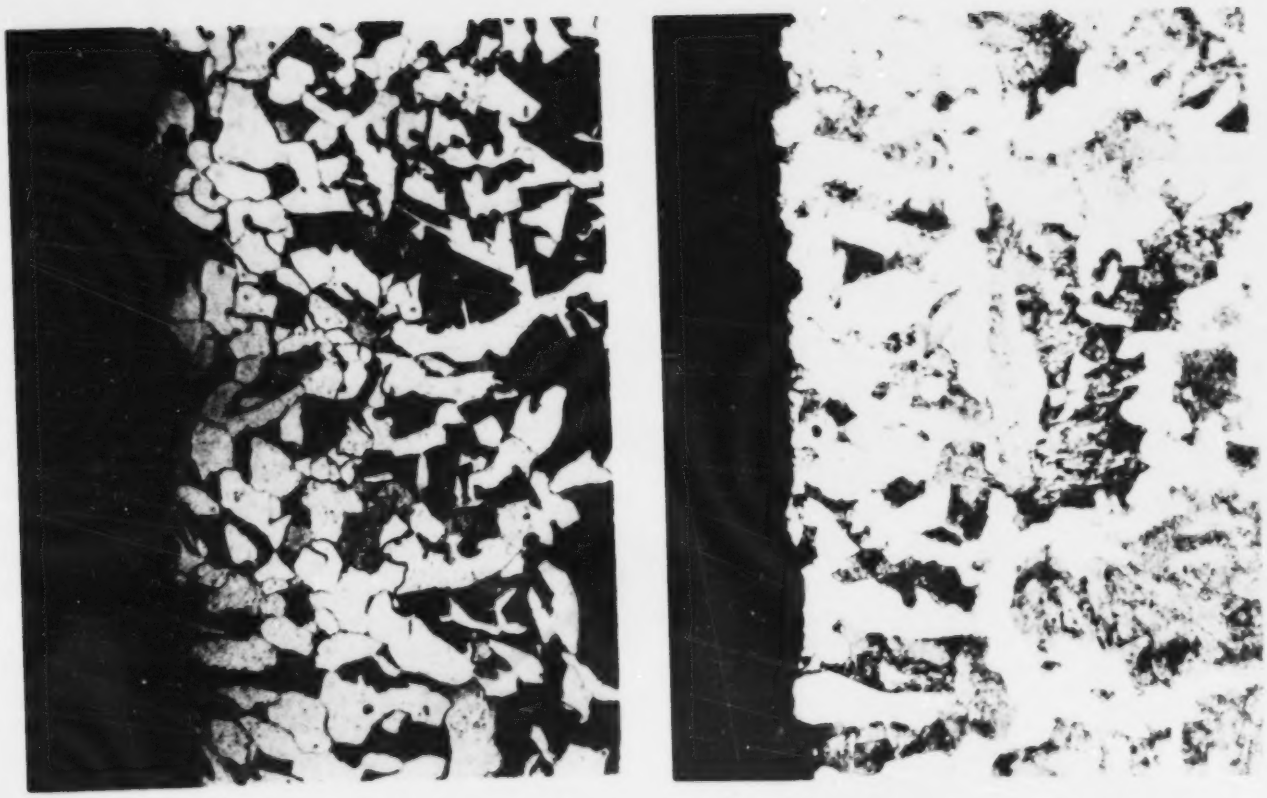

As-received coupon

Exposed Coupon

Etched sectional surfaces of the
as-received and exposed (Run #1c)
test coupons (Algoma K55)

FIGURE 13

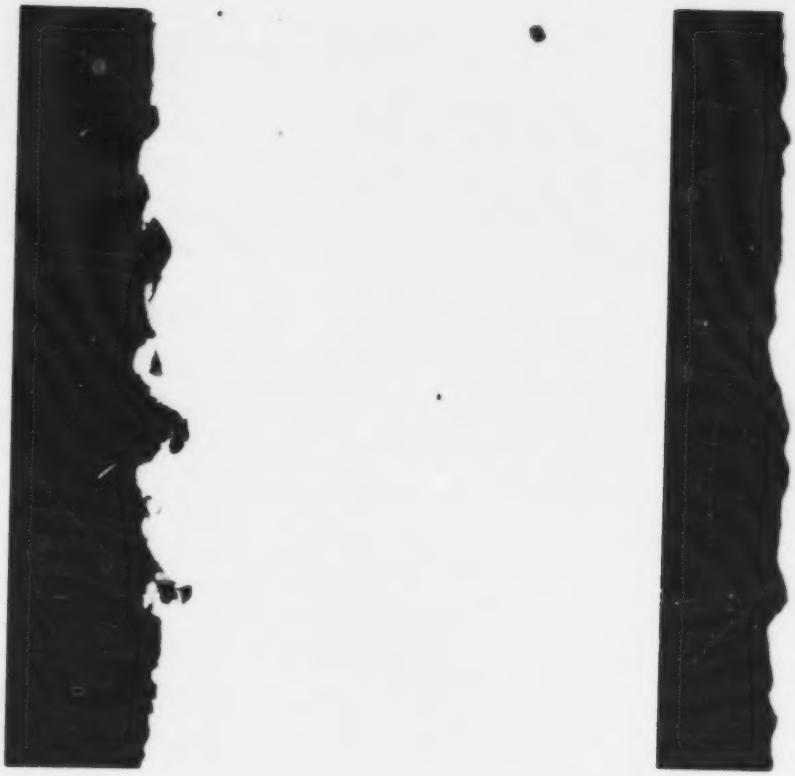

As-received Coupon

Exposed Coupon

Sectioned surfaces of the as-received and exposed
(Run #1c) Test Coupons
(Ipsco K55)

FIGURE 14

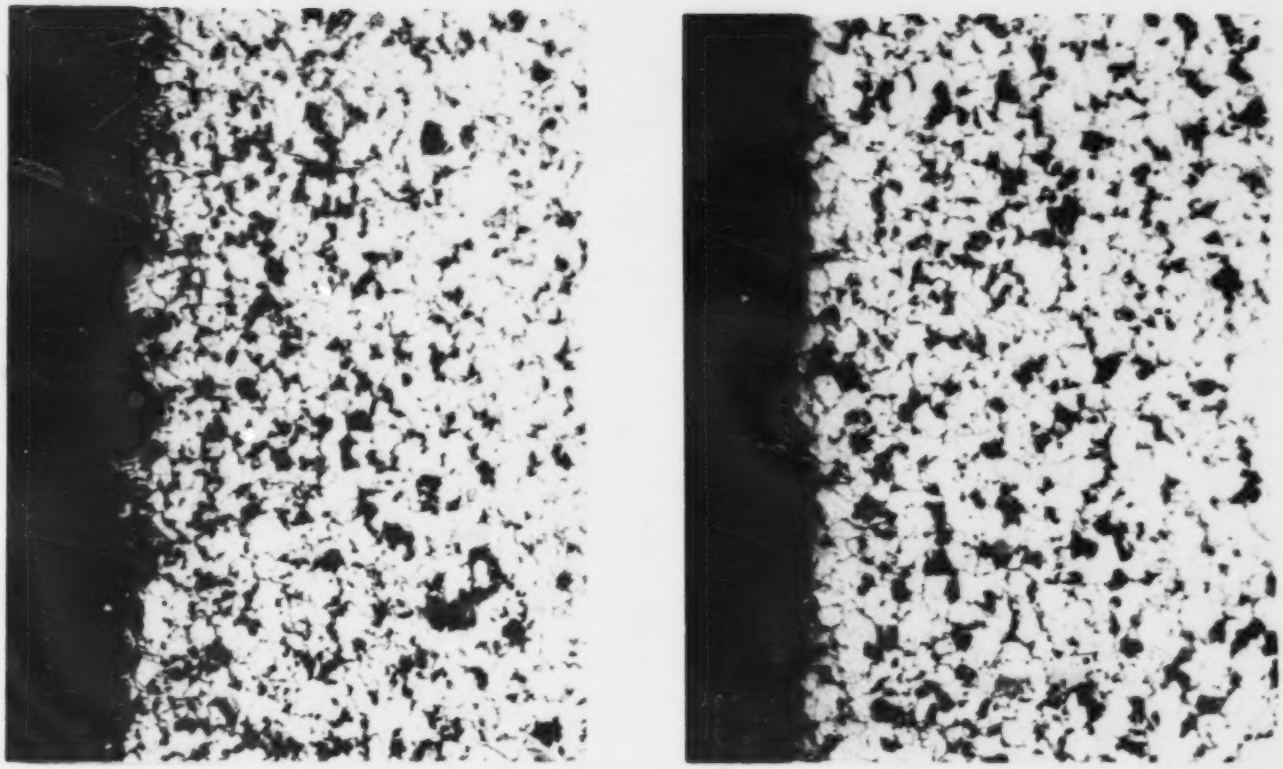

As-received Coupon

Exposed Coupon

Etched surfaces of the as-received and exposed
(Run #1c) test coupons
(Ipsco K55)

FIGURE 15

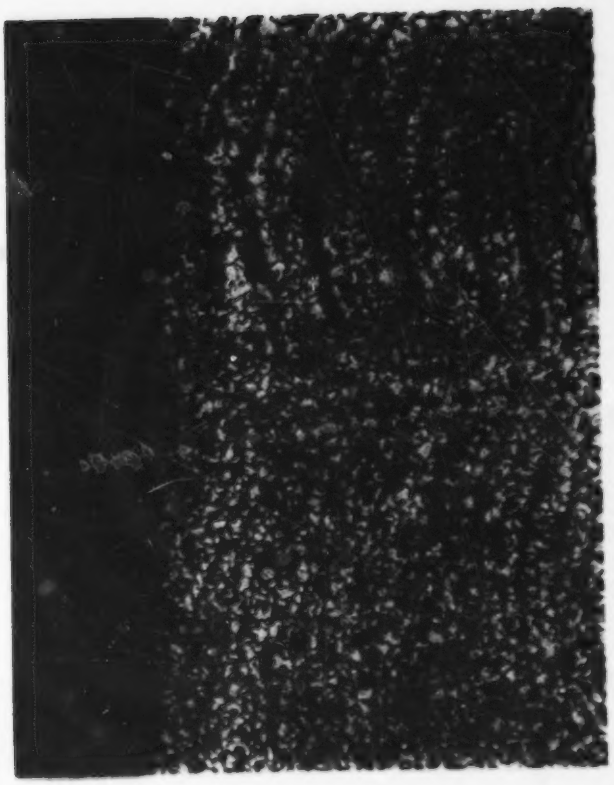

Etched surfaces of welded region of the exposed
(Run #1c) test coupons
(Ipsco K55)

Mag. 200 X

APPENDIX A

MOUNTING CONFIGURATIONS OF CARBON STEEL COUPONS ON TEFLON COUPON RACK

Figures 1 to 4 of Appendix A illustrate the mounting configuration of the coupons, for a particular experiment, on the upper and lower coupon tree. The number in brackets is the corrosion rate for the particular coupon. Please note the corrosion rates are greater for coupons of the same material mounted on the upper rack as compared to coupons mounted on the lower rack. This is consistent with a CO_2(aq) concentration gradient along the length of the autoclave.

FIGURE 1

Arrangement of Coupons on
Upper and Lower Coupon Racks
For Experiment 2. Numbers in
Brackets are Corrosion Rates (mm/yr)

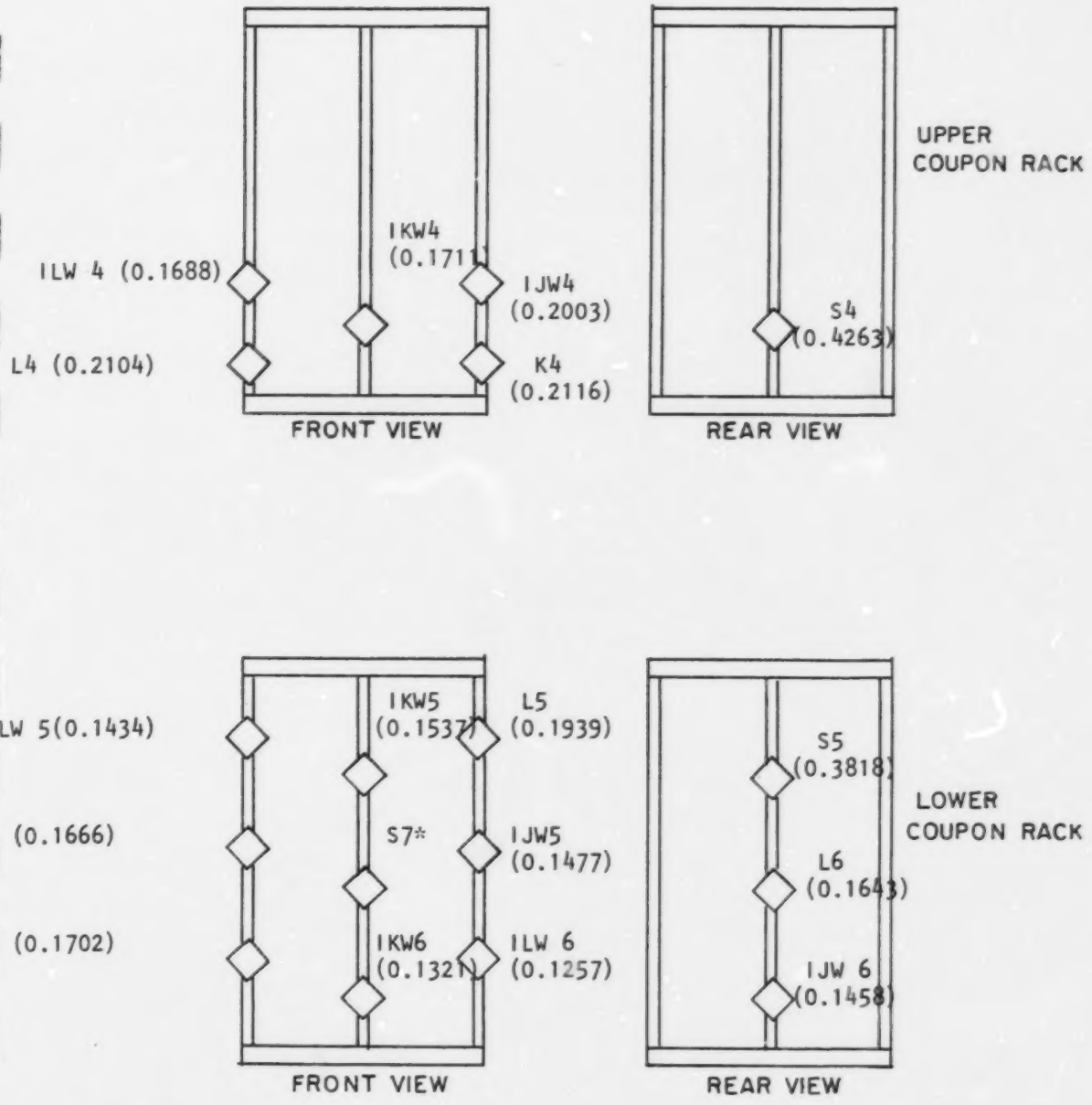

*S7 was damaged, therefore a corrosion rate was not determined for this coupon.

FIGURE 2

Arrangement of Coupon on
Upper and Lower Coupon Racks
For Experiment 3. Numbers in
Brackets are Corrosion Rates (mm/yr.)

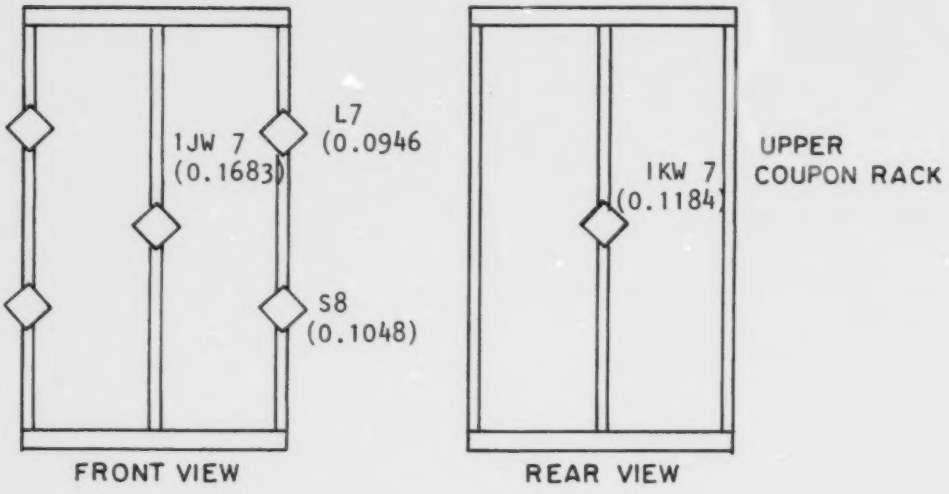

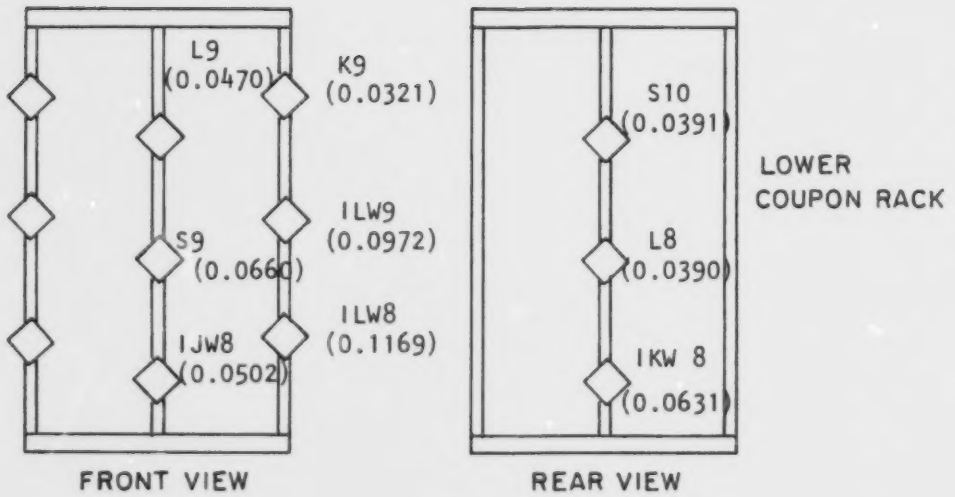

FIGURE 3

Arrangement of Coupon on
Upper and Lower Coupon Racks
For Experiment 4. Numbers in
Brackets are Corrosion Rates (mm/yr)

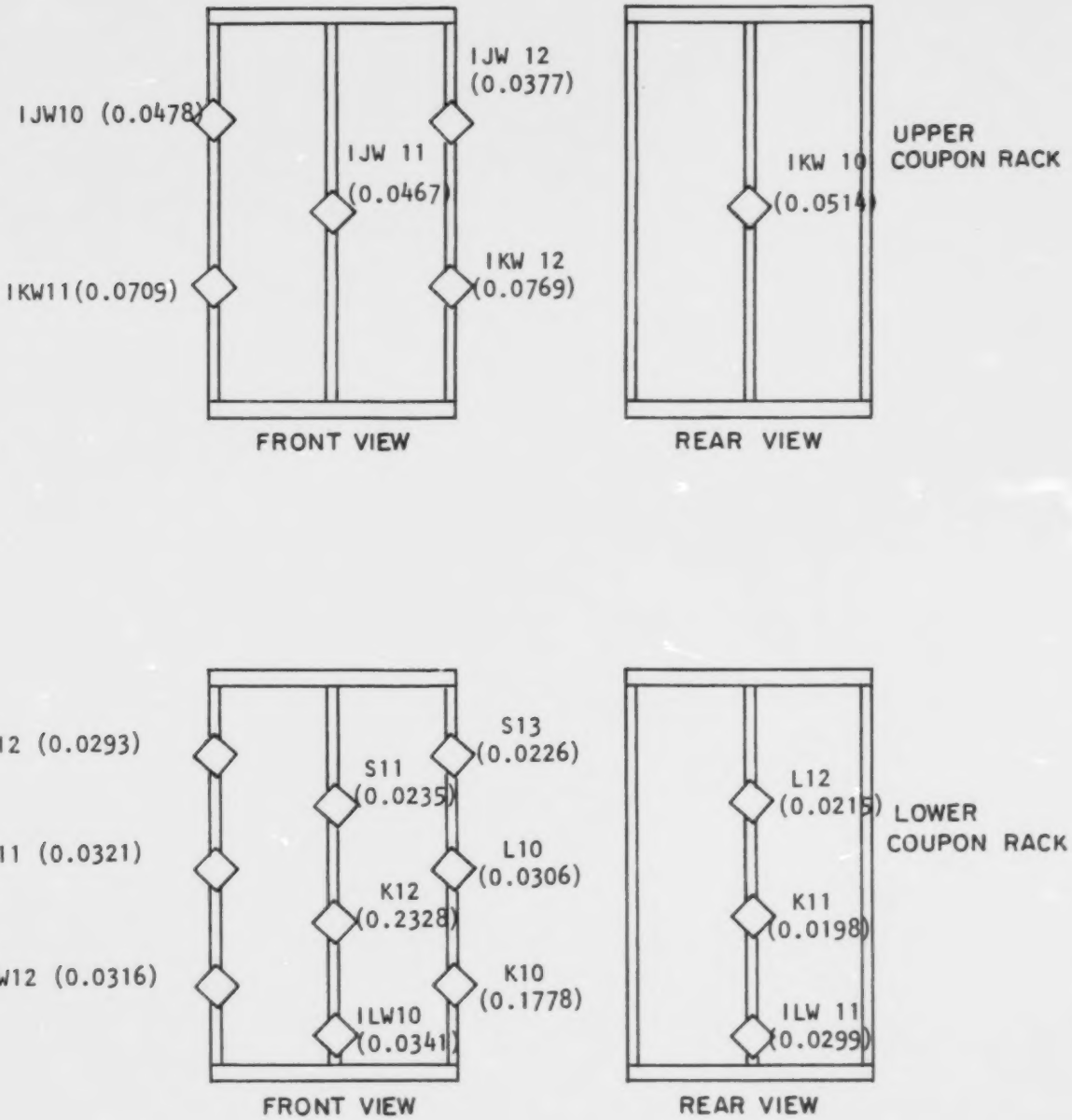

FIGURE 4

Arrangement of Coupon on
Upper and Lower Coupon Racks
For Experiment 5. Numbers in
Brackets are Corrosion Rates (mm/yr).

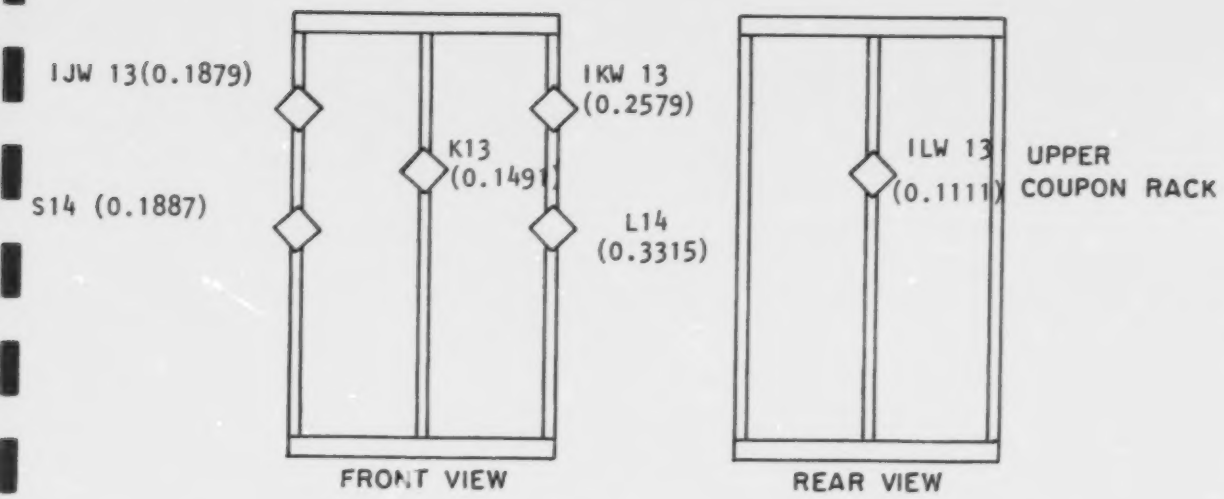

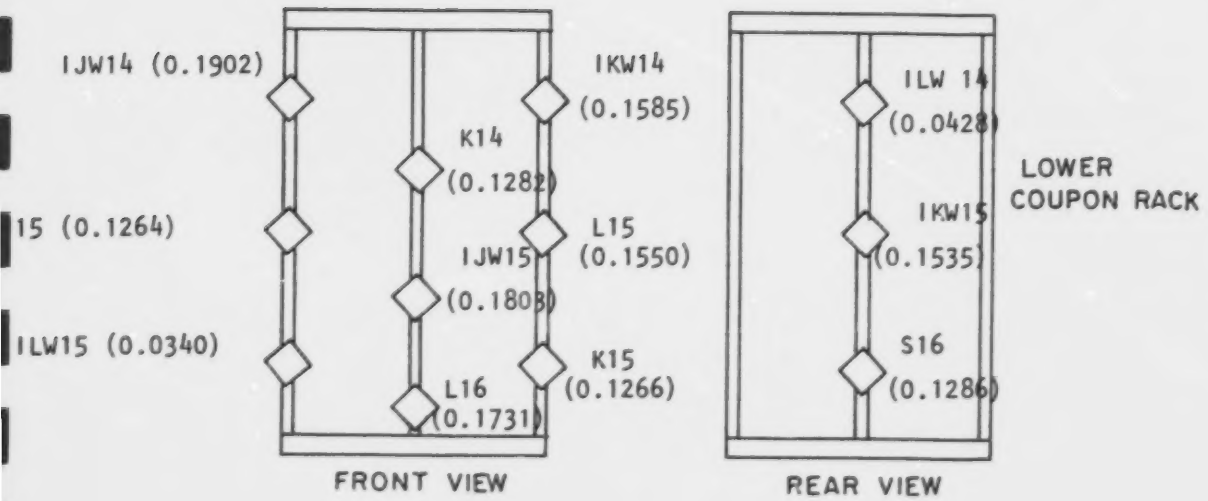

ONTARIO **RESEARCH**
FOUNDATION

Energy

energy conservation programs and analyses, thermal insulation design and evaluation, waste heat recovery, building energy systems and monitoring, heat storage systems and materials, thermoelectric generation, combustion technology, burner development, heat transfer analysis, solar systems monitoring, National Solar Test Facility, solar technology, wind power, coal, lignite and oil sands processing, alternate fuel utilization, battery and fuel cell technology, peat processing and utilization, fenestration measurements, heat pump development and test facilities, residential heating systems, air to air heat exchange test facility, photovoltaic devices, . . .

Environment

ambient air quality assessment, environmental impact assessments, long-range transport of atmospheric pollutants, precipitation chemistry, particulate characterization studies, emission inventories, source sampling, odour emission and control, asbestos measurement and control, occupational health and safety studies, diesel emission control technology, air pollution control, pesticide residues, trace metal analysis, trace organic analysis, radionuclide analysis, mutagenic testing, noise and vibration analysis, radiation measurements, particulate identification and measurement, water surveys, water purification, industrial and municipal wastewater treatment, membrane separation techniques, wet oxidation, solid waste treatment and recovery, hazardous waste treatment and disposal, indoor air quality assessments, priority pollutant analysis, landfill technology, . . .

Materials

building materials, plastics, composites, metals, glass and ceramics, wood and wood composites, biomaterials, adhesives and printing inks, fibres, yarns, fabrics and geotextiles, leather, organic and inorganic chemicals, specification development, quality assurance, mechanical, chemical and thermal properties, test method development, failure analysis, fire and flammability, glass-metal seals, metal and alloy powders, metallography, materials characterization, materials characterization by optical and electron microscopy and X-ray microanalysis, photovoltaic materials, materials corrosion resource centre, corrosion properties and control, bacterial corrosion, coatings and sealants, rubber technology, X-ray analysis, cement and concrete, soils and aggregates, gypsum, body armour testing, footwear, paper-making materials, roofing and waterproofing, waste material stabilization and solidification, . . .

Products & Processes

clothing, footwear and industrial textile products, knitting technology, thin and thick film systems, microelectronics development, fibre optics, instrumentation, bioengineering, ultrasonic and fluid shear devices, microwave drying, transportation and equipment testing, mathematical stress and vibration analysis, product, equipment and machinery design & development, fuel emulsification, organic analysis and characterization, chemistry of foodstuffs, pulp and paper processes, ceramics processing, metallurgical process development, powder metal technology, packaging applications, technical and economic evaluations, industrial engineering applications, process control, enzyme analysis, electrical testing, radioactive surveys, industrial microbiology, biotechnology, technical and management skills development seminars, paper products, absorbent consumer products, detergent and cosmetic formulation, metal chemical analysis, flash hydropyrolysis of coal, electroplating, . . .

Resources

mineral processing, hydro and pyrometallurgical processing of ferrous and non-ferrous ores, coal evaluation, coal ash utilization and product development, asbestos processing and applications, non-metallic minerals/industrial minerals processing and utilization, uranium processing, forest utilization, utilization of forest and agricultural wastes, utilization of industrial, mining and domestic wastes, energy and chemicals from biomass, in-plant waste reduction, mineralogical services, mining and metallurgical waste disposal, . . .

ONTARIO RESEARCH FOUNDATION • SHERIDAN PARK, MISSISSAUGA, ONTARIO, CANADA L5K 1B3 • (416) 822-4111 • TELEX 06-982311

CONTRACT SERIAL NUMBER 1SQ 85-00099
DSS REQUISITION NUMBER 23440-5-9032
CONTRACTOR: C&M Engineering Ltd.

Report No. 57-10731
Contract No. 03SQ-23440-5-9032

Effect of CO_2/H_2S on Seamless And ERW Tubular Goods

For
C & M Engineering Ltd.
2220-39th Ave. N.E.
Calgary, Alberta
T2E 6P7

Attention: Mr. Colin Duncan

Prepared By:
J. D. Tyrer, Ph.D.
S. H. Lo, Ph.D.
R. T. Lassau, M.Sc.

Metals Technology Centre

April 30, 1988

ONTARIO RESEARCH FOUNDATION
SHERIDAN PARK RESEARCH COMMUNITY
MISSISSAUGA, ONTARIO, CANADA L5K 1B3 • (416) 822-4111 • TELEX 06-982311

61 pp

MICROMEDIA

WE, THE ONTARIO RESEARCH FOUNDATION, STIPULATE THAT THIS DOCUMENT IS SUBJECT TO THE FOLLOWING TERMS AND CONDITIONS
1. ANY PROPOSAL CONTAINED HEREIN WAS PREPARED FOR THE CONSIDERATION OF THE ADDRESSEE ONLY. ITS CONTENTS MAY NOT BE USED BY NOR DISCLOSED TO ANY OTHER PARTY WITHOUT OUR PRIOR WRITTEN CONSENT.
2. ANY TESTING, INSPECTION OR INVESTIGATION PERFORMED BY US WILL BE CONDUCTED IN ACCORDANCE WITH NORMAL PROFESSIONAL STANDARDS. NEITHER WE NOR OUR EMPLOYEES SHALL BE RESPONSIBLE FOR ANY LOSS OR DAMAGE RESULTING DIRECTLY OR INDIRECTLY FROM ANY DEFAULT, ERROR OR OMISSION.
3. ANY REPORT, PROPOSAL OR QUOTATION PREPARED BY US REFERS ONLY TO THE PARTICULAR MATERIAL, INSTRUMENT OR OTHER SUBJECT REFERRED TO IN IT. NO REPRESENTATION IS MADE THAT SIMILAR ARTICLES WILL BE OF LIKE QUALITY.
4. NO REPORT ISSUED BY US SHALL BE PUBLISHED IN WHOLE OR IN PART WITHOUT OUR PRIOR WRITTEN CONSENT.
5. OUR NAME SHALL NOT BE USED IN ANY WAY IN CONNECTION WITH THE SALE, OFFER OR ADVERTISEMENT OF ANY ARTICLE, PROCESS OR SERVICE.
6. WE RESERVE THE RIGHT NOT TO COMMENCE AND/OR CONTINUE ANY WORK UNTIL PAYMENT ARRANGEMENTS SATISFACTORY TO US ARE ESTABLISHED.

C & M Engineering Ltd.
Corrosion and Materials Specialists

August 22, 1988

Energy, Mines and Resources Canada
Assistant Director - Minerals
Research Program Office
Canada Centre for Mineral & Energy Technology
568 Booth Street
OTTAWA, Ontario K1A 0G1

ATTENTION: Mr. R. Winston Revie

RE: EFFECT OF CO_2/H_2S ON SEAMLESS AND ERW TUBULAR GOODS
CONTRACT NO. 03S-Q-23440-5-9032

Dear Sir:

The enclosed report presents the results of the extended corrosion research conducted on Canadian oilfield steel products exposed to a series of acid gas environments.

The experimental evidence presented in this study has demonstrated that as little as 10 mol percent H_2S in the CO_2/H_2S gas produces marked increases in the corrosion rates. Also, we have demonstrated that the presence of calcium and bicarbonate ions in the contacting brine solution reduces the corrosion rate under these severe conditions at 150°C and 4000 psig.

We have found some general departure from the literature on certain aspects of the anticipated corrosion rates and the effects of temperature, gas composition and solution chemistry.

The steel products which have been tested are all production run materials from Canadian pipe mills. There has been no sensitivity demonstrated by the ERW long seam nor has either the seamless or welded product shown any evidence of catastrophic corrosion rates. This is a further encouraging aspect of the results which deserves some particular attention since it indicates that useful service life can be offered by the low alloy carbon steels.

2220 - 39th Avenue N.E., Calgary, Alberta T2E 6P7 Telephone (403) 250-7081 Telex 03-827924 Fax (403) 291-5681

The tests have been carefully controlled and documented so that the reader may understand precisely what was done and how the tests were interpreted.

The report concludes that although these results are encouraging, there remains to be an important number of other field variables which would require examination in bringing the work forward to a field application.

C & M Engineering and our Industrial and Research partners wish to express our gratitude for the fine co-operative assistance provided by Canmet and more particularly, your office. We are also indebted to the Federal Government support for our project and the co-operative fiscal management provided by the staff of the Department of Supply & Services.

Yours very truly,

for Colin Duncan, P. Eng.

CD:ck
attach.

Please package this form with documents sent for inclusion in Microlog. We will return it to you with the documents and our document order numbers filled in for your reference.

Series	Number	Extra Comments	Date Sent to MML	Microlog Order Number
CONTRACT REPORTS				
OSQ	83-00195	Pt. A,B,C,D&E	Feb 3/89	
OSQ	85-00093		"	
OSQ	85-00164	Final report	"	
OSQ	84-00205		"	
OSQ	85-00211	Final report	"	
	59118-01-SQ		"	
	69061-01-SZ	Final report	"	
	69064-01	Summ. & Final	"	
	69100-01-SQ	Final report	"	
	69121-01-SQ	Vol. 1 & 2	"	
(french)	69137-01-SQ	rapport d'etudes	"	
(english)	69137-01-SQ	Study report	"	
	69138-01-ST		"	
	69161-01-ST			
	69163-01-SQ	Final report	"	
	69175-04-SQ	Vol. 1 ph. 1 & 2		
f	69187-01-SQ	Final report	"	
	69189-01-ST	Final report	"	
	69197-01-ST		"	
	79009-01-ST	phase II	"	
	79039-02-SQ	phase I & II & des. spec.	"	
	79045-01-SS	Final Progress Rpt."		
	79067-09-SQ		"	
	79152-01-SQ	Final Report	"	
	79226-01-SQ	Pro. Pt. 1 & 2	"	

see next page

SENT FROM/RETURN TO: Corinne Langdon, CANMET, 562 Booth St. Room 20C

Ottawa, Ontario, K1A 0G1

Same

Contact: Same Phone: (613) 992-4207

MICROMEDIA LIMITED: 144 Front Street West, Toronto, Ontario, M5G 2L7

Please package this form with documents sent for inclusion in Micrologue. We will return it to you with the documents and our document order numbers filled in for your reference.

Series	Number	Extra Comments	Date Sent to MML	Micrologue Order Number
CONTRACT REPORTS (cont'd)				
	89003-01-SG		Feb.3/89	
ISQ	85-00099	In two parts	"	

SENT FROM/RETURN TO: see page 1

Contact: _____ Phone: _____

MICROMEDIA LIMITED: 144 Front Street West, Toronto, Ontario, M5G 2L7

TABLE OF CONTENTS

		Page
	EXECUTIVE SUMMARY	1
1.	INTRODUCTION	3
2.	OBJECTIVES	3
3.	PROCEDURES	4
	3.1 Autoclave System	4
	3.2 Experimental Procedure	4
	3.3 Coupon Preparation	5
	3.4 X-ray Diffraction Analysis	7
	3.5 Corrosion Rates	7
	3.6 Contributing Sources of Error in the Corrosion Rates of Coupons of the Same Steel Grade Exposed to a Chemical Environment	8
	3.7 Metallography	9
4.	RESULTS AND DISCUSSION	10
	4.1 Corrosion Rate Data for Coupons Exposed to a 150°C Brine Solution in Equilibrium with a Gas Phase of 50% CO_2, 10% H_2S and 40% N_2 at 4000 psia - Experiment 1	10
	4.2 Corrosion Rate Data for Coupons Exposed to a 150°C Brine Solution in Equilibrium with a Gas Phase of 50% CO_2, 50% H_2S at 4000 psia - Experiment 2	10
	4.3 Corrosion Rate Data for Coupons Exposed to a 150°C Brine Solution in Equilibrium with a Gas Phase of 50% CO_2, 50% H_2S at 4000 psia - Experiment 3	11
	4.4 Corrosion Rate Data for Coupons Exposed to a 100°C Brine Solution in Equilibrium with a Gas Phase of 50% CO_2, 50% H_2S at 4000 psia - Experiment 4	11
	4.5 Discussion of Corrosion Rate Data	12

Page

5. SUMMARY AND CONCLUSIONS 16

6. COMPARISON OF CORROSION RATES FROM LABORATORY AND FIELD STUDIES 17

7. FUTURE STUDIES 18

BIBLIOGRAPHY

APPENDIX I

Report No. 57-10731
C & M Engineering Ltd.

EXECUTIVE SUMMARY

It is important to the oil and gas industry, from a technical and economic basis, to understand the parameters which control the corrosion processes of carbon dioxide and hydrogen sulphide on tubular goods in oil and gas reservoirs. This report describes the results of a corrosion investigation directed towards determining the corrosion rates and metallurgical effects on ERW and seamless tubular carbon steel coupons exposed to aqueous carbon dioxide/hydrogen sulphide/brine environments in the 100°C - 150°C temperature range.

The results of this study and the Phase I study have demonstrated that, in the 100°C - 150°C temperature range, the following conclusion may be made.

(i) The presence of hydrogen sulphide at levels in excess of 10 mole percent of the CO_2/H_2S gas phase produces corrosion rates for carbon steels in brine solution that are noticeably higher than those produced in a CO_2/brine environment.

(ii) Increases in H_2S gas phase concentrations from 10 mole percent to 50 mole percent increase corrosion rates by a factor of 2 - 3 in brine solutions where HCO_3^- and Ca^{2+} were absent.

(iii) The Ca^{2+} and/or HCO_3^- ions can potentially reduce corrosion in H_2O/CO_2 brine solutions.

(iv) Corrosion of carbon steels in CO_2/H_2S/brine solutions saturated with H_2S is a result of oxidation of the metal by H_2S; CO_2 may not contribute significantly to the corrosion process through direct participation.

(v) The corrosion rates of the seamless and welded grades of steel, submitted for study in this program, were similar. This implies that differences between the materials due to chemistry, heat treatment and the inclusion of welds were not significant to distinguish them by their corrosion behaviour under the experimental conditions in this study. General corrosion was the only type of corrosion observed.

RESUME

D'un point de vue technique et economique , il est important pour l'industrie petrolifere de comprendre les parametres qui controlent les processus de corrosion dans les canalisations et dans les conduits a l'interieur des reservoirs ; corrosion due a l'action de l'anhydride carbonique (ou acide carbonique) et de l'hydrogene sulfure.

Ce rapport decrit les resultats des etudes effectuees en vue de determiner le taux de corrosion et les consequences metallurgiques sur des echantillons de tubes d'acier au carbone sans soudure et de ERW soumis a des milieux acide carbonique / hydrogene sulfure / eau salee evoluant dans un intervalle de temperature compris entre 100 et 150 degres Celcius.

Les resultats de cette etude et de l'etude PHASE 1 ont demontre que , dans le champ de temperatures 100-150 Deg C, les conclusions suivantes peuvent etre tirees:

(i) lorsque la teneur en mole d'hydrogene sulfure du compose gazeux CO2/H2S excede 10 %, on peut noter que le taux de corrosion des aciers au carbone est plus important dans une solution d'eau salee que dans une solution CO2/eau salee.

(ii) lorsque la teneur en mole d'hydrogene sulfure varie de 10 % a 50 % le taux de corrosion, lui, est multiplie par 2 a 3 fois dans une solution d'eau salee ou les ions HCO_3^- et Ca^{2+} n'existent pas.

(iii) les ions HCO_3^- et/ou Ca^{2+} peuvent potentiellement reduire la corrosion dans les solutions H2S/CO2/eau salee.

(iv) la corrosion de l'acier dans les solutions H2S/CO2/eau salee ,saturees en H2S ,est le produit de l'oxydation du metal par l'hydrogene sulfure; l'acide carbonique ne contribue pas directement au phenomene de corrosion d'une maniere significative.

(v) le taux de corrosion de l'acier avec ou sans soudure , soumis a l'etude dans ce programme , sont similaires. Ceci implique que les differences entre les materiaux dues, a la chimie , aux traitements calorifiques, et a la presence de soudures ne sont pas significatives pour les distinguer par leur comportement vis a vis de la corrosion sous les conditions experimentales de cette etude. La corrosion generale a ete le seul type de corrosion observe.

1. INTRODUCTION

The corrosion of materials under the influence of carbon dioxide and hydrogen sulphide is of great interest to the oil and gas industry. Either one or both of these gases are naturally occurring in oil and gas reservoirs. In addition, enhanced oil recovery methods such as steam stimulation and in situ combustion expose downhole tubular materials to significant levels of produced hydrogen sulphide and carbon dioxide at temperatures well in excess of the natural reservoir temperature. This results in excessive corrosion in both injection and production wells and surface facilities. A possible extension of the useful life of downhole tubular materials, if only by 50 percent, would achieve considerable reduction in capital and operating costs. Thus, it is important from a technical and economic basis, to understand the parameters which control the corrosion processes of carbon dioxide and hydrogen sulphide on tubular goods.

This report describes the results of a corrosion investigation directed towards determining the corrosion rates and metallurgical effects of tubular carbon steel coupons exposed to aqueous carbon dioxide/hydrogen sulphide/brine environments in the 100°C - 150°C temperature range at a total pressure of 4,000 psia.

2. OBJECTIVES

The objectives of the program were to characterize and elucidate the mechanism of corrosion damage affecting the performance of both ERW and seamless tubular goods exposed to CO_2/H_2S brines in the 100°C to 150°C temperature range. In particular, the effect of adding H_2S gas to a CO_2/brine solution, on the corrosion of seamless and ERW carbon steel coupons was determined by comparing the results of this Phase II program to those of the Phase I study, (Report No. 57-10486, Contract No. 03SQ-233440-5-9032, Effect of CO_2 on Seamless and ERW Tubular Goods, January 27, 1987). Whether sodium bicarbonate and calcium chloride inhibit the corrosion of seamless and ERW goods in H_2S/CO_2/brine solutions was also determined.

3. PROCEDURES

3.1 Autoclave System

All experiments were conducted in a 2-gallon Hastelloy C autoclave. The autoclave was equipped with gas and liquid sampling ports, a gas injection line and magnetic stirring to provide solution agitation. The autoclave was heated by a 3-zone heater that provided temperature control to ± 2°C of the set point. The autoclave has maximum operating pressure and temperature limits of 5,000 psi (34.47 kpa), and 500°C respectively. Figure 1 is a schematic drawing of the autoclave used in the experiments.

3.2 Experimental Procedure

For the purpose of the corrosion experiments, three (3) coupons of each steel grade were mounted on a Teflon coupon tree as illustrated in Figure 2. The chemical composition of each steel grade is listed in Table 1. Each coupon was suspended on stainless steel wire that was coated with Teflon tubing. This ensured that each coupon did not contact any dissimilar metal surfaces. Experiments were conducted either in a brine solution prepared according to ASTM D 1141 or in a solution identical to that of ASTM D 1141 except that $NaHCO_3$ and $CaCl_2$ were replaced by an equivalent number of moles of NaCl. Table 2 lists the concentrations of the various brine solution components.

Sufficient brine was used to cover all coupons with the aqueous phase during the experiments, such that the volume/area ratio was 10 ml/cm^2. It is important to note that the brine was boiled for one half hour prior to each experiment to minimize dissolved oxygen levels. Care was taken to ensure that evaporative losses did not occur, and therefore the concentration of HCO_3^- was not altered during this procedure. After boiling, nitrogen gas was bubbled through the cooled brine solution to prevent the reabsorption of oxygen.

A total of four (4) autoclave experiments were conducted and the specific conditions of each experiment are summarized in Table 3.

Experiments 2 and 3 were terminated after 13 days. This was due to the rupture of the Bourdon tube in the pressure gauge, during experiment 2 and failure of the rupture disc safety head assembly during experiment 3. To permit a direct comparison of test results, it was decided to run experiment 4 for thirteen days rather than 21 days.

The procedure used for each experiment is described in the following sequence of events. The coupons and oxygen free brine were placed in the autoclave which was then sealed. The oxygen, in the air space above the liquid brine, was removed by evacuating the autoclave and repressurizing the system with oxygen free nitrogen to a total pressure of 15 psia. The autoclave was then heated to the required temperature, while the solution was stirred vigorously to achieve equilibrium. A compressor was used to achieve the required gas mixture. The total operating pressure for each experiment was 4,000 psia.

Gas chromatography was used in each test to ensure that the gas phase concentrations of carbon-dioxide and hydrogen sulphide were ±5 volume percent of the required levels. Dissolved oxygen was determined using a dissolved oxygen test Kit, (Chemetrics Inc.), and was found to be less than 1 ppm for all experiments.

3.3 Coupon Preparation

The ERW and seamless carbon steel coupons were received by Ontario Research from C & M Engineering of Calgary. The ERW material was originally provided by IPSCO (Regina, Saskatchewan) and consisted of steel grades IJW55, IKW55 and IL80. The seamless material was provided by Algoma Steel (Sault Ste. Marie, Ontario) and consisted of steel grades K55, L80 and S0095. The chemical composition of the test materials is listed in Table 1. Ontario Research received a total of 25 numbered coupons of each steel grade prepared by C & M Engineering. These coupons were used in the Phase I study and experiments 1 and 2 of this study. To complete the Phase II study, C & M Engineering supplied Ontario Research with additional coupons. These coupons were used in experiments 3 and 4

of the Phase II program. All coupons were prepared by cutting them to uniform dimensions and providing surface and edge finishes suitable for the program.

The coupons had approximate dimensions of 3.5 cm X 3.5 cm X 0.8 cm. The IJW55 samples were derived from 5½" O.D., (13.97 cm), and 0.275", (0.70 cm), wall thickness ERW casing. The IJW55 is a medium carbon, low sulphur steel in a full body normalized condition. The IKW55 samples were derived from 7" O.D., (17.78 cm), and 0.272", (0.69 cm), wall thickness ERW casing. The IKW55 is a medium carbon, low sulphur steel microalloyed with molybdenum and vanadium, and in a full body normalized condition. The IL80 samples were derived from 7" O.D., (17.78 cm), and 0.362", (0.92 cm) wall thickness ERW casing. The IL800 is a medium carbon, low sulphur steel microalloyed with vanadium and molybdenum, and in quenched and tempered condition.

The Algoma Steel samples were derived from 9.5" O.D., (24.13 cm), casing. The edges had been finished to 320 grit and a glass bead technique had been used to remove mill scale from the coupon surfaces. Figures 3 to 8 illustrate the geometry and surface features of the coupons. It is important to note that the coupons were prepared from actual pipe stock. This produced coupons with curved surfaces, surface metallurgical conditions, and weld profiles that more closely simulate field applications.

For the purpose of determining corrosion rates using weight loss measurements, the coupons were degreased in acetone, weighed and dimensioned to determine surface areas. All coupons were stored in a desiccator (with drying agent) until required for a particular experiment. This eliminated any potential corrosion of the carbon steel surfaces by humid air.

3.4 X-ray Diffraction Analysis

X-ray diffraction analyses were conducted using a Philips recording diffractometer to identify crystalline phases present in the corrosion products. The filmed inner surface of one coupon removed from a particular experiment was used for these analyses. Note, the scope of the program was not sufficient for X-ray analyses to be conducted on all steel types exposed to each of the chemical environments. All X-ray spectra were carefully examined to ensure that all chemical compounds, (i.e. metal oxides, metal hydroxides, metal sulphides, metal carbides, and metal carbonates), were detected. Table 4 summarizes the results of the X-ray diffraction analysis.

3.5 Corrosion Rates

The corrosion rates were calculated from weight loss data. The measured weight losses and the calculated corrosion rates are presented in Tables 5 to 10.

Corrosion rates were calculated from weight loss data using the following equation:

$$\text{Corrosion rate } \frac{\text{mm}}{\text{yr}} = \frac{87.6\ W}{DAt}$$

87.6	=	constant to provide corrosion rates in mm/yr.
W	=	weight loss in milligrams
D	=	density in g/cm³ (taken as 7.86 g/cm³ for all steel grades).
A	=	coupon area in cm².
t	=	experimental time in hours.

The corrosion product on the coupons was removed by first cleaning them in a mild detergent, followed by short exposure (5 seconds) to a dilute (10%) hydrochloric acid solution. The acid cleaning was continued

until most, if not all, of the product had been removed. This was determined by examining the coupon surface with an optical microscope and, where necessary, continuing the cleaning process until all the coupon surface was judged to be free of corrosion products.

3.6 Contributing Sources of Error in the Corrosion Rates of Coupons of the Same Steel Grade Exposed to a Chemical Environment

The corrosion rate data reported in Tables 5 to 10 indicates some minor variation in the corrosion rates of coupons of the same steel grade, exposed to identical environments. As well, Table 11 provides a summary of the average corrosion rates and 90% confidence limits (t - distribution), for the various steels exposed to different chemical environments. This observed variation is due in part to the following.

(i) The curved geometry of the coupons made it difficult to measure coupon length and width. As a result, it is estimated that the relative error in the coupon areas is ± 10%. This is based on an absolute error of ± 1 mm in the length and width dimensions of each coupon.

(ii) The surface finish of the coupons was variable. Although glass bead abrasion was used to remove mill scale etc., it was noted that both flat surfaces of the coupons had irregular non-smooth topographies. The extent of the irregularity in surface finish was not consistent even among coupons of the same steel grade. In particular, coupons with very rough surfaces would be expected to have increased corrosion rates in comparison to coupons with smoother surfaces. This also introduces an error in the surface area measurement. It is difficult to estimate the magnitude of this error on the corrosion rates.

(iii) The welds of the ERW materials were not uniform and there were weld trim areas which were raised slightly above adjacent base

metal areas on the coupons. Variations in coupon surface areas due to variations in the weld areas are also difficult to measure.

Large variations (2-3 orders of magnitude) in the corrosion rate data, for the same steel grade exposed to identical chemical environments, were not observed in this study. However, such a variation was observed in the Phase I study "Effects of CO_2 on Seamless and Tubular Goods". It was postulated that a CO_2 concentration gradient existed along the length of the autoclave. The gradient, if real, was possibly produced by insufficient stirring of the brine solution. Adjustment of the coupon racks allowed the magna-drive system to be operated at speeds of 1,000 rpm. This eliminated concentration gradients in the brine solution, and thus eliminated variations in corrosion rates.

3.7 Metallography

Six different types of steels were investigated in this corrosion study. The different grades of steels were K55, L80 and S0095 from the Algoma Steel Company and K55, J55, L80 from the IPSCO Steel Company. The materials provided by IPSCO contained an ERW weld in the centre of each coupon. The chemical compositions of the above materials are listed in Table 1.

Among the Algoma Steels, the K55 has a pearlitic microstructure, while the L80 and S0095 are low alloy steels with quenched and tempered martensitic microstructures. In the case of IPSCO materials, both the IJW55 and IKW-55 have fine pearlitic microstructures, whereas the ILW-80 shows a quenched and tempered martensitic microstructure.

Due to the method of manufacturing, the Algoma Steel samples show a notably rougher surface, even after the surface preparation treatment. Attempts at modifying the surface with acid pickling were unsuccessful. Consequently, a longer glass beading treatment was applied to the Algoma samples in an attempt to produce a more complete removal of residual mill scale.

Metallographic examinations were performed on all test coupons subjected to the corrosive environments listed in Table 3. The exposed coupons were initially examined for general surface features, followed by a detailed metallographic examination on their cross-section in both polished and etched conditions.

In general, an adherent surface coating was found on all samples exposed to CO_2/H_2S brine test environments. This coating, shown in Figure 9 on a test coupon photographed after the first series of test runs, was found to consist of pyrrhotite, $Fe_{1-x}S$.

The observations made on the test coupons that were subjected to the different test environments are listed in Appendix I.

4. RESULTS AND DISCUSSION

4.1 Corrosion Rate Data for Coupons Exposed to a 150°C Brine Solution in Equilibrium with a Gas Phase of 50% CO_2, 10% H_2S and 40% N_2 at 4000 psia - Experiment 1

Experiment number 1 consisted of exposing the steel coupons to an ASTM D 1141 brine solution, (free of $NaHCO_3$ and $CaCl_2$), in equilibrium with a gas phase as noted above, for a period of 21 days. Corrosion rate data, at 0.4 mm/yr. on average, are similar among all steel grades, except the IKW55 material which had corrosion rates averaging 0.2 mm/yr. The materials have good corrosion resistance in this test environment. The major corrosion product was pyrrhotite, $Fe_{1-x}S$. Some marcasite, FeS_2, was also detected as a minor product.

4.2 Corrosion Rate Data for Coupons Exposed to a 150°C Brine Solution in Equilibrium with a Gas Phase of 50% CO_2, 50% H_2S at 4000 psia - Experiment 2

Experiment number 2 consisted of exposing the test coupons to an ASTM D 1141 brine solution, (free of $NaHCO_3$ and $CaCl_2$), with a gas phase composition rich in H_2S as noted above. Originally, the experiment was to be conducted for a 21 day period. On the thirteenth

day, the Bourdon tube in the pressure gauge ruptured and the coupons were exposed to oxygen This resulted in partial oxidation of the iron sulphide surface deposits to hydrated iron oxides. Rather than continue the experiment, it was decided to calculate corrosion rates for the first 13 days of the experiment. The corrosion rates are similar for all materials and range from 0.8 to 1.5 mm/yr. Again, X-ray diffraction analysis indicated that the primary corrosion product was pyrrhotite $Fe_{1-X}S$. In this environment, the corrosion resistance of the various materials has decreased. Table 14 correlates corrosion resistance and corrosion rate.

4.3 Corrosion Rate Data for Coupons Exposed to a 150°C Brine Solution in Equilibrium with a Gas Phase of 50% CO_2, 50% H_2S at 4000 psia - Experiment 3

Experiment 3 involved exposing the test coupons to an ASTM D 1141 brine solution, (with $NaHCO_3$ and $CaCl_2$ present in the brine), in a gas phase composition as noted above, for a period of 21 days. The experiment was terminated after 13 days due to a failure of the safety head assembly on the 13th day. The corrosion rates of all materials in this environment were between 0.3 and 0.6 mm/yr. The major product of corrosion was pyrrhotite, $Fe_{1-X}S$. This experiment was identical to experiment 2, except that the brine contained HCO_3^- and Ca^{2+} ions. The decrease in corrosion rates may be indicative of a corrosion inhibition process involving one or both of these ionic species.

4.4 Corrosion Rate Data for Coupons Exposed to a 100°C Brine Solution in Equilibrium with a Gas Phase of 50% CO_2, 50% H_2S at 4000 psia - Experiment 4

The final experiment consisted of exposing test coupons to an ASTM D 1141 brine solution, (with $NaHCO_3$ and $CaCl_2$ present in the brine), in a gas phase composition as noted above, for a period of 13 days in order to provide a comparison with the shorter tests 2 and 3.

The materials all exhibited good corrosion resistance in this environment as corrosion rates varied between 0.2 and 0.5 mm/yr. The

major corrosion product was pyrrhotite $Fe_{1-X}S$. The observed decrease in corrosion rates (compare the average corrosion rates for experiment 2 with those of experiment 4) can be attributed to the lower temperature and/or the presence of the HCO_3^- and Ca^{2+} ions.

4.5 Discussion of Corrosion Rate Data

All coupons were covered with a black solid film after exposure to their respective environments. Table 4 is a summary of the corrosion products found on coupons after each experiment. The X-ray diffraction data clearly indicate that the major corrosion product in each experiment was pyrrhotite, $Fe_{1-X}S$. Metal carbonates such as $FeCO_3$ were not detected. Hydrogen sulphide is largely responsible for corrosion of the carbon steel coupons. The corrosion process may be represented by the following reaction:

$$H_2S + Fe_{1-X} \rightarrow Fe_{1-X}S + H_2 \uparrow.$$

Due to the failure of the Bourdon tube, during experiment 2, oxygen leaked into the autoclave. This resulted in oxidation of the iron sulphides, present on the coupon surfaces, to iron oxide hydroxide. Both α and β forms were detected by X-ray diffraction analysis.

$$2FeS_2 + 5.5O_2 + H_2O \rightarrow 4SO_2 + 2FeO.OH.$$

The experiment was terminated at this time, (13 days), as it was not understood how the presence of FeO.OH would influence corrosion rates if the experiment had been continued.

The corrosion rate data are presented in Tables 5 to 10, and Table 11 provides an average corrosion rate and 90% confidence limit from the t-distribution. Upon examination of the data the following conclusions can be drawn:

(i) for a particular experiment, the corrosion rates for the seamless and ERW materials are similar. The notable exception is the corrosion rate of the IKW55 material, of experiment 1, which differed by a factor of two from the corrosion rate of the other materials. This indicates that the differences in chemical composition, and structural features, including the welded seam, between the materials, has a minimal influence on the corrosion rates in H_2S/CO_2 brine solutions;

(ii) comparison of the corrosion rate data for experiments 1 and 2 (both experiments involved the use of the ASTM D 1141 brine with $NaHCO_3$ and $CaCl_2$ replaced by an equivalent number of moles of NaCl), indicates that an increase in the H_2S gas phase concentration results in a substantial increase in corrosion rates for all steel types. This again emphasized the fact that the coupon's morphological features cannot be selectively differentiated in these environments;

(iii) comparison of the corrosion rates of experiments 2 and 3 (Table 12) indicates that the presence of HCO_3^- and Ca^{2+} ions in the brine inhibits corrosion of the carbon steel surfaces. Both of these experiments were conducted at 150^oC with a gas phase composition of 50% H_2S and 50% CO_2. The presence of HCO_3^- and Ca^{2+} in the brine reduced corrosion rates by a factor of from 2 to 3. It is also noteworthy that the corrosion rates of experiment 3, (50% CO_2, 50% H_2S, 150^oC, HCO_3^-/Ca^{2+} ions present) are similar to those of experiment 1, (50% CO_2, 10%H_2S 40% H_2, 150^oC, HCO_3^-/Ca^{2+} ions absent). Apparently the HCO_3^- and Ca^{2+} ions inhibit corrosion to the extent that the potential corrosiveness of a 50% H_2S system is reduced to that of a 10% H_2S system;

(iv) the corrosion rates of experiment 4 (50% H_2S, 50% CO_2, 100°C, HCO_3^-/Ca^{2+} present in the brine), are less than those of experiment 2, (50% H_2S, 50% CO_2, 150°C, HCO_3^-/Ca^{2+} replaced by NaCl). It is not posssible, with the present set of experimental data, to determine if this decrease is largely due to the lower temperature of experiment 4 or to the presence of HCO_3^- and Ca^{2+} ions, or both.

It is not clear how the HCO_3^- and the Ca^{2+} ions are inhibiting corrosion of the steel surfaces. However, it is possible that during the initial heat-up of the autoclave (before the addition of CO_2 and H_2S gas) the HCO_3^- ion participates in the formation of a protective siderite ($FeCO_3$) layer. Note, experiment 2 of the Phase I CO_2 study confirmed that the HCO_3^- ion present in the brine produced a siderite component that represented approximately 70 percent of the corrosion product produced in the absence of CO_2 and H_2S gases. If this film is present and is less than 10 microns thick, it would not be easily detected by X-ray diffraction. Auger microscopy studies would be necessary to detect the presence of a thin metal carbonate film on the coupon surfaces produced by the initial exposure to a brine solution containing $NaHCO_3$.

Comparison of the corrosion rates of this CO_2/H_2S Phase II study with those of the CO_2 Phase I study (see Tables 11 and 13) clearly suggest that the presence of hydrogen sulphide increases the extent of corrosion of the test materials. The results of the Phase I study indicated that passivation of the coupon surfaces was occurring due to the formation of a hard non-permeable siderite film. The film formed in the presence of H_2S consisted mostly of pyrrhotite, $Fe_{1-x}S$, and does not passivate the coupon surfaces to the same degree as siderite.

The corrosion results of this study differ somewhat from the corrosion rate data reported by Ikeda et al.[1] These researchers studied the variation in corrosion of pure iron in the presence of CO_2/brine solutions with increasing amounts of H_2S added. The experiments were conducted in the 25°C to 250°C temperature range. Generally, it was observed that for all levels of H_2S, the corrosion rates at 100°C were greater than those at 150°C. Increasing the concentration of H_2S reduced the overall corrosion rate at 100°C. Figure 10 illustrates the variation in corrosion rates with temperature and H_2S concentration. These researchers also determined that the major corrosion product was iron carbonate.

The results of this Phase II study show that hydrogen sulphide, not carbon dioxide, is primarily responsible for the corrosion produced on the steel surfaces. This was determined by X-ray diffraction analysis of the filmed surfaces. It is reasonable to conclude then that as H_2S levels are increased in CO_2/brine solutions, the H_2S eventually becomes the major influence on the corrosion of carbon steel surfaces. It is important to note the concentrations of H_2S used in the current program. Ikeda used H_2S levels of less than 500 ppm, whereas in the present study the brine solution was essentially saturated with H_2S. At some point, therefore, as the concentration of H_2S increases in CO_2/brine solutions, the H_2S must become principally responsible for the overall corrosion process.

It is also interesting that the corrosion rates, reported by Ikeda, increase in the vicinity of 100°C and then decrease at higher temperatures. This is a result of the contribution of carbon dioxide to the corrosion, and this effect has been documented in the literature by Schmitt.[2]

This effect was not observed in this study. The corrosion rates generated at 100°C, (experiment number 4) are less than those generated at 150°C, (experiment number 2). As stated earlier, it is not clear if this effect is due to the lower temperature or potential corrosion inhibition by the HCO_3^- and Ca^{2+} ions.

The metallographic results and discussion can be found in Appendix I.

5. SUMMARY AND CONCLUSIONS

The results of this study and the Phase I study have demonstrated that, in the 100°C to 150°C temperature range, the following conclusion may be made.

(i) The presence of hydrogen sulphide at levels in excess of 10 mole percent of the CO_2/H_2S gas phase produces corrosion rates for carbon steels in brine solution that are noticeably higher than those produced in a CO_2/brine environment.

(ii) Increases in H_2S gas phase concentrations from 10 mole percent to 50 mole percent increase corrosion rates by a factor of 2 - 3 in brine solutions where HCO_3^- and Ca^{2+} were absent.

(iii) The Ca^{2+} and/or HCO_3^- ions can potentially reduce corrosion in H_2O/CO_2 brine solutions.

(iv) Corrosion of carbon steels in CO_2/H_2S/brine solutions saturated with H_2S is a result of oxidation of the metal by H_2S; CO_2 may not contribute significantly to the corrosion process through direct participation.

(v) The corrosion rates of the seamless and welded grades of steel, submitted for study in this program, were similar. This implies that differences between the materials due to chemistry, heat treatment and the inclusion of welds were not significant to distinguish them by their corrosion behaviour under the experimental conditions in this study. General corrosion was the only type of corrosion observed.

6. COMPARISON OF CORROSION RATES FROM LABORATORY AND FIELD STUDIES

In general, corrosion rates from field studies are greater than those measured in the laboratory. This is due to the increased complexity of real as opposed to artificial brines. Real brines may contain organic acids capable of participating in the overall corrosion process. In addition, flow rates in oil well and gas tubing are much higher (of the order of metres/second) as compared to the flow rates generated in a stirred autoclave. As well, flow cycling of the wells introduces stresses and thermal cycling, which are not considered in laboratory experiments. The data reported for this experimental study do not account for the influence of thermal and flow cycling on corrosion rates.

The corrosion rate data collected for experiment 1 suggest that the steel grades have corrosion resistance to 150°C brines that have gas phase compositions of less than 10 mole per cent. This suggests that these materials may be suitable for use in steam stimulation or in situ combustion projects in which high downhole temperatures but low hydrogen sulphide levels are encountered. However, the results of experiment2 suggest that the materials may have a limited applicability for certain hot sour gas wells with high levels of H_2S. These materials may be suitable for this application if corrosion can be reduced by some well bore chemical treatment, surface coating, alloy material selection, or by some other unspecified operational control.

7. FUTURE STUDIES

The results of these studies are very interesting and very encouraging for the products tested. However, there are many gaps in the information collected so far; in particular in the temperature H_2S/CO_2 concentration profiles which need to be filled in for Algoma and Ipsco to have a completed data sheet with which to sell Canadian tubular goods to domestic and foreign markets. Certainly continued work in this area is necessary and highly desirable.

In addition, there is an indication that HCO_3^-/Ca^{2+}, in some combination, acts as an inhibitor to metal corrosion in H_2S/CO_2 environments. This effect should be investigated for the potential it may have as a field remedy for accelerated corrosion in the severe environments encountered in sour gas wells. Real brines, which may contain organic acids capable of participating in the overall corrosion process, should be added for study here.

Finally, low velocity is another of the important downhole field parameters that influences corrosion/erosion rates on metal surfaces, and therefore should be added as a study parameter in the next phase of this program.

This added information will provide Ipsco and Algoma with the data necessary to market their downhole tubular steels with confidence, and will generally serve the oil and gas industry with a tested product capable of reducing their production costs.

R. T. Lassau, Manager
Materials Corrosion/
Metals Investigations

0692k

BIBLIOGRAPHY

1. Ikeda, A., Veda, M., and Mukai, S., "Influences of Environmental Factors on Corrosion in CO_2 Source Well", Advances in CO_2 Corrosion, Vol. 2: Proceedings of the Corrosion '84 Symposium in CO_2 Corrosion in the Oil and Gas Industry, p 1.

2. Schmitt, G., "Fundamental Aspects of CO_2 Corrosion", Advances in CO_2 Corrosion, Vol. 1: Proceedings of the Corrosion '83 Symposium in CO_2 Corrosion in the Oil and Gas Industry, p 10.

TABLE 1

CHEMICAL COMPOSITIONS OF TEST MATERIALS

		C	Mn	P	S	Si	Cr	Mo	Al
Algoma	K55	0.47	1.01	0.018	0.015	0.30	0.05	0.02	0.046
	L80	0.27	1.36	0.023	0.017	0.31	0.10	0.06	0.046
	S0095	0.29	1.30	0.023	0.016	0.31	0.09	0.06	0.037
IPSCO	IJW-55	0.25	1.38	0.011	0.005	0.25	-	-	0.027
	IKW-55	0.288	0.96	0.010	0.002	0.26	-	0.159	0.007
	ILW-80	0.265	0.92	0.012	0.003	0.25	-	0.166	0.052

TABLE 2

BRINE COMPOSITION

(ASTM D 1141)

The brine solution was prepared by combining 245.34 g of NaCl and 40.94 g of anhydrous Na_2SO_4 in 8 L of water. A 200 mL aliquot and a 100 mL aliquot of stock solutions No. 1 and No. 2, respectively, were added to this solution. The total solution volume was diluted to 10.0 L and the pH adjusted to 8.2 with 0.1 N NaOH.

Stock Solution No. 1

$MgCl_2.6H_2O$	555.6 g/L
$CaCl_2$ (anhydrous)	57.9 g/L
$SrCl_2.6H_2O$	2.1 g/L

Stock Solution No. 2

KCl	69.5 g/L
$NaHCO_3$	20.1 g/L
KBr	10.1 g/L
H_3BO_3	2.7 g/L
NaF	0.3 g/L

TABLE 3

AUTOCLAVE EXPERIMENTS

Experiment Number	
1	50% CO_2, 10% H_2S, 40% N_2, 150°C, 4,000 psia total pressure; 21 days
2	50% CO_2, 50% H_2S, 150°C, 4,000 psia total pressure; 13 days
3	50% CO_2, 50% H_2S, 150°C, 4,000 psia total pressure; 13 days
4	50% CO_2, 50% H_2S, 100°C 4,000 psia total pressure; 13 days

The brine used in experiments numbered 1 and 2 is per ASTM D 1141, except that $NaHCO_3$ and $CaCl_2$ were replaced by an equivalent number of moles of NaCl.

TABLE 4

COUPON DEPOSIT COMPOSITION FROM
X-RAY DIFFRACTION ANALYSIS

Experiment Number	Coupon Deposit Composition
1	Major component pyrrhotite, $Fe_{1-x}S$, (90%); trace ~ 10% FeS_2, Marcasite
2	Major component, (50-60%) pyrrhotite, $Fe_{1-x}S$; akaganeite, β-FeO(OH) (20-30%); and lepidocrocite, $Fe_2O_3.H_2O$, (10%).
3	Major component pyrrhotite, $Fe_{1-x}S$, (90-95%); marcasite, FeS_2, (1-2%)
4	Major component pyrrhotite, $Fe_{1-x}S$, (95%); marcasite, FeS_2 (5%)

Description of Tables 5 - 10

Weight gain column - refers to difference in weights between "as-received" and autoclaved conditions of coupon. Gains are due to surface filming.

Weight loss column - refers to difference in weights between "as-received" and descaled conditions of coupons. Losses are due to general metal corrosion and incorporation of metal into film.

TABLE 5

CORROSION RATE DATA FOR K-55 SEAMLESS SPECIMENS

Coupon No.	Experiment No.	Weight Gain (mg)	Weight loss (mg)	Corrosion Rate (mm/yr.)
K-19	1	274.8	677.1	0.41
K-21	1	267.6	674.0	0.37
K-22	2	454.2	1140.3	0.97
K-23	2	537.7	1344.4	1.06
K-24	2	509.7	1674.0	1.51
K-1-2	3	169.5	444.5	0.36
K-2-2	3	182.5	483.8	0.38
K-3-2	3	160.2	466.4	0.37
K-16-2	4	64.4	335.9	0.29
K-18-2	4	-167.2*	459.9	0.40
K-20-2	4	38.2	386.9	0.34

*Indicates a weight loss

TABLE 6

CORROSION RATE DATA FOR L-80 SEAMLESS SPECIMENS

Coupon No.	Experiment No.	Weight Gain (mg)	Weight loss (mg)	Corrosion Rate (mm/yr)
L-17	1	278.6	727.7	0.41
L-19	1	311.7	682.1	0.38
L-20	1	330.6	643.7	0.36
L-21	2	386.5	1282.5	1.07
L-22	2	520.0	1398.9	1.10
L-24	2	556.2	831.1	1.03
L-1-2	3	184.8	374.9	0.37
L-2-2	3	196.1	359.0	0.36
L-3-3	3	203.4	362.4	0.36
L-13-2	4	70.3	331.4	0.26
L-14-2	4	59.7	312.9	0.25
L-15-2	4	-30.9*	409.4	0.33

*Indicates a weight loss

TABLE 7

CORROSION RATE DATA FOR S0095 SEAMLESS SPECIMEN

Coupon No.	Experiment No.	Weight Gain (mg)	Weight Loss (mg)	Corrosion Rate (mm/yr.)
S-18	1	305.8	735.9	0.41
S-19	1	417.7	920.6	0.46
S-20	1	352.5	709.5	0.37
S-21*	2	379.4	1864.0	1.38)
S-22	2	503.7	1130.1	0.86)
S-23	2	1245.9	974.4	0.78)
S-1-2	3	208.1	518.8	0.37
S-2-2	3	153.4	646.5	0.46
S-2-3	3	219.4	515.5	0.37
S-13-2	4	49.6	304.0	0.25
S-14-2	4	-173.5**	595.3	0.48
S-15-2	4	36.6	281.5	0.23

*Coupon data suspect, so not included in t-distribution calculations (Table 11)

**Indicates a weight loss

TABLE 8

CORROSION RATE DATA FOR IJW-55 ERW SPECIMENS

Coupon No.	Experiment No.	Weight Gain (mg)	Weight Loss (mg)	Corrosion Rate (mm/yr.)
IJW-19	1	234.5	352.7	0.38
IJW-20	1	234.4	528.6	0.40
IJW-21	1	288.6	608.5	0.39
IJW-22	2	284.6	895.7	0.83
IJW-23	2	327.7	1028.1	1.11
IJW-24	2	458.5	1121.8	1.04
IJW-1-2	3	172.8	549.3	0.44
IJW-2-2	3	38.9	772.4	0.61
IJW-3-2	3	189.8	438.8	0.35
IJW-13-2	4	112.3	336.9	0.31
IJW-14-2	4	110.1	335.9	0.29
IJW-15-2	4	94.9	392.5	0.35

TABLE 9

CORROSION RATE DATA FOR IKW-55 ERW SPECIMEN

Coupon No.	Experiment No.	Weight Gain (mg)	Weight Loss (mg)	Corrosion Rate (mm/yr.)
IKW-17	1	248.8	258.4	0.17
IKW-18	1	222.3	269/3	0.19
IKW-19	1	248.5	309.2	0.22
IKW-16	2	378.2	1154.8	1.09
IKW-20	2	325.6	1061.6	1.03
IKW-21	2	397.3	1001.7	1.01
IKW-1-2	3	5.6	738.1	0.56
IKW-2-2	3	69.4	679.5	0.50
IKW-3-2	3	213.7	493.4	0.40
IKW-16-2	4	118.5	346.2	0.31
IKW-17-2	4	98.6	315.2	0.28
IKW 18-2	4	73.9	276.5	0.25

TABLE 10

CORROSION RATE DATA FOR ILW-80 ERW SPECIMEN

Coupon No.	Experiment No.	Weight Gain (mg)	Weight Loss (mg)	Corrosion Rate (mm/yr.)
ILW-18	1	274.4	577.8	0.39
ILW-19	1	264.3	448.6	0.33
ILW-20	2	476.5	978.4	1.08
ILW-21	2	523.2	1040.2	1.09
ILW-22	2	517.6	1051.3	1.07
ILW-2-2	3	178.7	564.6	0.43
ILW-3-2	3	199.5	466.5	0.34
ILW-13-2	4	104.9	377.9	0.32
ILW-14-2	4	99.5	319.4	0.28
ILW-15-2	4	111.1	321.7	0.27

Report No. 57-10731
C & M Engineering Ltd.

TABLE 11

AVERAGE CORROSION RATES (mm/yr) AND
90% CONFIDENCE LIMIT FROM t-DISTRIBUTION

Carbon Steel	Experiment 1	2	3	4
K55	0.39*	1.18 ± 0.49	0.37 ± 0.02	0.34 ± 0.09
L80	0.38 ± 0.04	1.07 ± 0.06	0.36 ± 0.01	0.28 ± 0.07
S0095	0.41 ± 0.08	0.82	0.40 ± 0.09	0.37 ± 0.23
IJW55	0.39 ± 0.02	0.99 ± 0.25	0.47 ± 0.14	0.32 ± 0.05
IKW55	0.19 ± 0.04	1.04 ± 0.07	0.47 ± 0.14	0.28 ± 0.05
ILW80	0.36	1.08 ± 0.02	0.39	0.29 ± 0.04
Experimental Conditions	50%CO_2, 10% H_2S 40% N_2,4,000 psia, 150°C, 21 days	50% CO_2, 50% H_2S, 4,000 psia, 150°C, 13 days	50% CO_2,50% H_2S, 4,000 psia, 150°C, 13 days	50% H_2S, 50% CO_2, 4,000 psia, 100°C, 13 days

NOTE: Experiments 1 and 2 utilized an ASTM D 1141 brine in which the $NaHCO_3$ and $CaCl_2$ were replaced by an equivalent number of moles of NaCl.

TABLE 12

RATIO OF THE AVERAGE CORROSION RATES
FOR EXPERIMENTS NUMBERED 2 AND 3

Carbon Steel Type	Ratio of Average Corrosion Rates (Experiment Number 2/ Experiment Number 3)
K55	3.2
L80	2.9
S0095	2.0
IJW55	2.1
IKW55	2.2
ILW80	2.8

TABLE 13*

AVERAGE CORROSION RATES (mm/yr) AND 90% CONFIDENCE LIMIT CALCULATED FROM t-DISTRIBUTION

(Phase I - CO_2 Investigation)

Carbon Steel	Experiment Number 2	3	4	5
K55	0.1828 ± 0.0421	0.0494 ± 0.0438	0.2953	0.1346 ± 0.0211
L80	0.1895 ± 0.0392	0.0602 ± 0.0505	0.0281 ± 0.0096	0.2198 ± 0.1636
S0095	0.4041	0.0699 ± 0.0556	0.0251 ± 0.0061	0.1479 ± 0.0595
IJW55	0.1646 ± 0.0521	0.0879 ± 0.1173	0.0441 ± 0.0084	0.1861 ± 0.0087
IKW55	0.1523 ± 0.0329	0.0816 ± 0.0537	0.0664 ± 0.0224	0.1899 ± 0.0991
ILW80	0.1459 ± 0.0365	0.1446 ± 0.1109	0.0318 ± 0.0035	0.0626 ± 0.0711
Experimental Conditions	0% CO_2 100% N_2, 150°C 4000 psia 28 days	50% CO_2 50%, N_2, 150°C 4000 psia 28 days	50% CO_2, 50% N_2 100°C, 4000 psia 28 days	50% CO_2, 50% N_2 150°C, 4000 psia 28 days Note: Brine $NaHCO_3$ and $CaCl_2$ free

* See Phase I Report - Effect of CO_2 on Seamless and ERW Tubular Goods Contract No. 035Q233440-5-9032, January 27, 1987

TABLE 14

CORRELATION OF CORROSION RESISTANCE AND CORROSION RATE

Relative Corrosion Resistance	Corrosion Rate (mm/yr)
Outstanding	<0.02
Excellent	0.02 - 0.1
Good	0.1 - 0.5
Fair	0.5 - 1.0
Poor	1.0 - 5.0
Unacceptable	5+

NOTE: Data from this table were produced from Fontana, M. G. and Greene, N. D., "Corrosion Engineering", McGraw Hill Book Company, New York, 1978.

FIGURE 1

SCHEMATIC DRAWING
OF HASTELLOY-C AUTOCLAVE

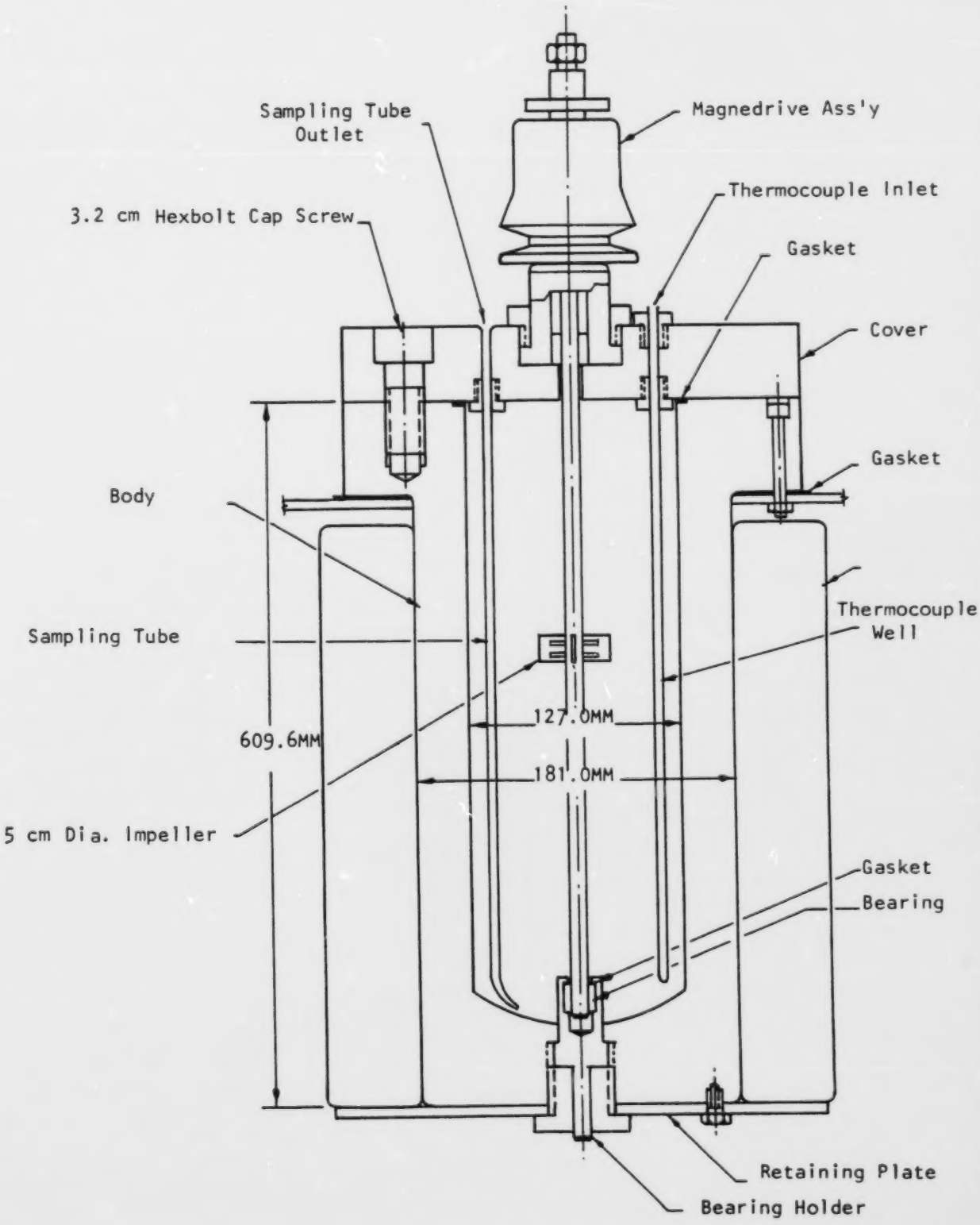

FIGURE 2

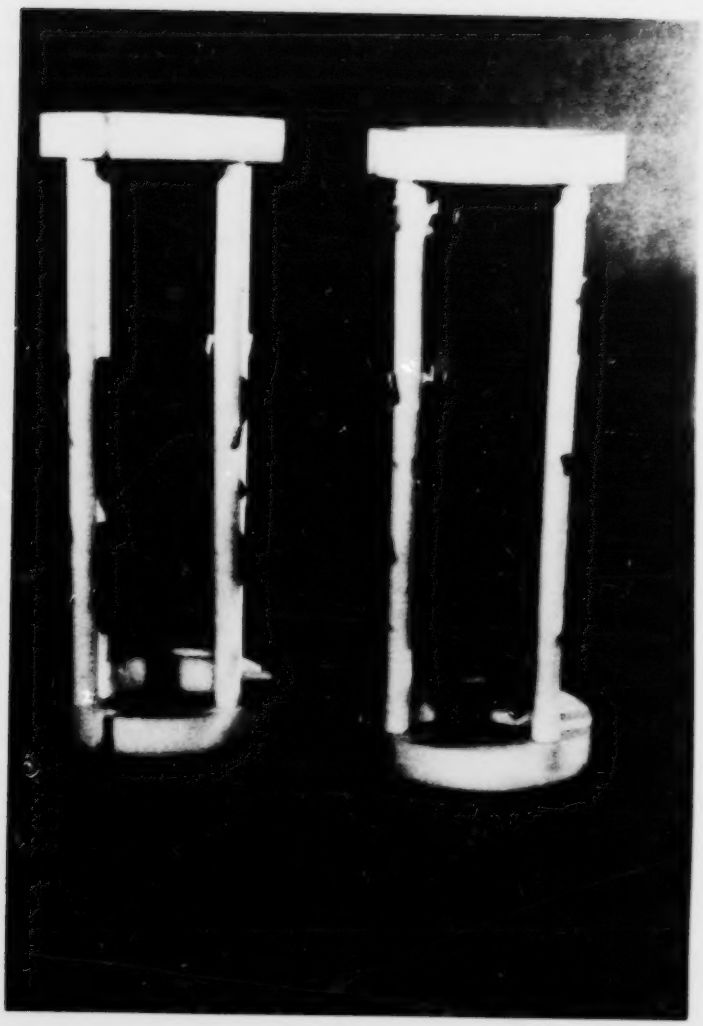

Teflon Coupon Racks
Used to Mount Seamless
and ERW Coupons

FIGURE 3

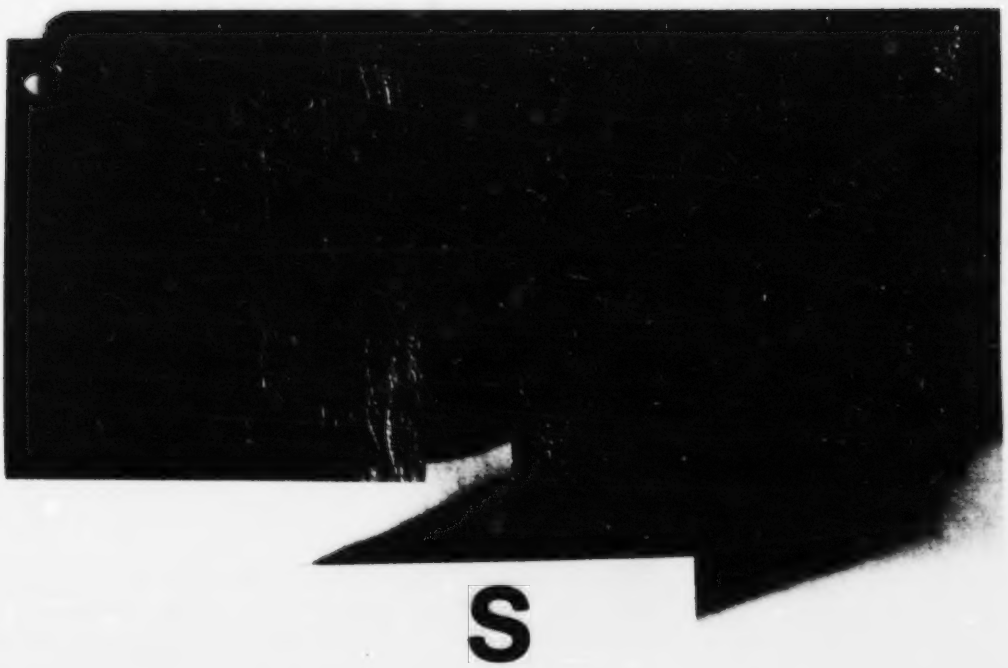

S

General Appearance of Seamless
S0095 Steel Coupons Provided By
Algoma Steel

FIGURE 4

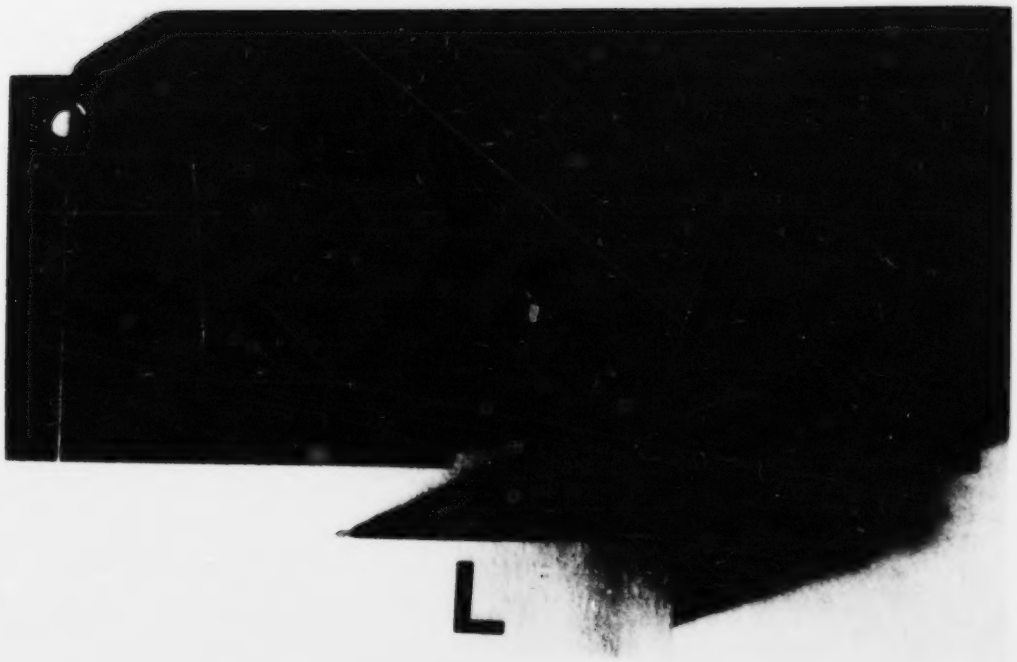

General Appearance of Seamless L80
Steel Coupons Provided by
Algoma Steel

FIGURE 5

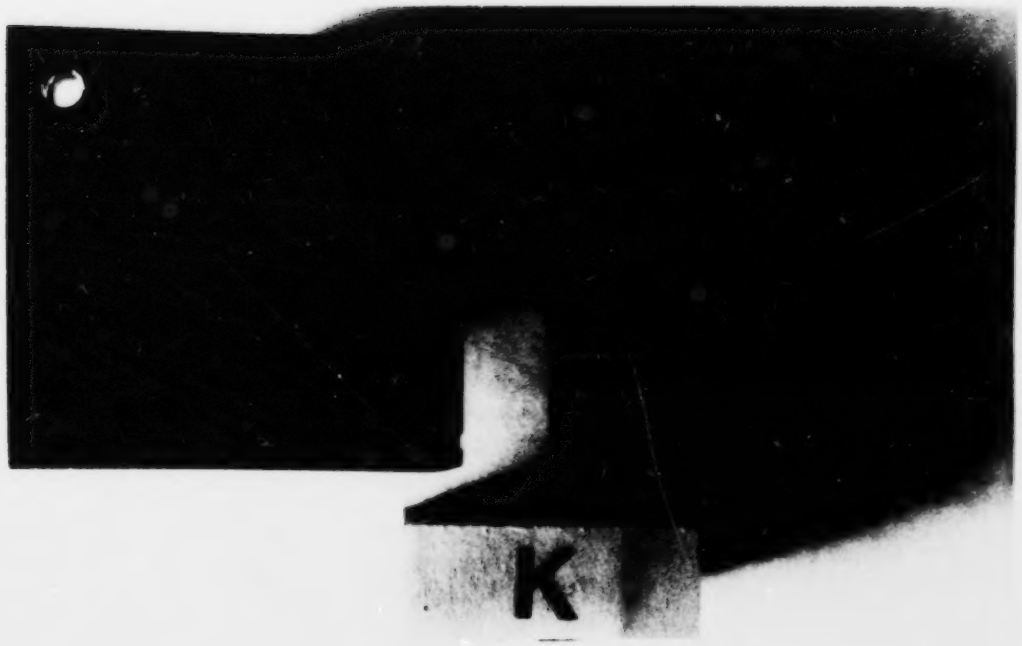

General Appearance of Seamless K55 Steel
Coupons Provided by Algoma Steel

FIGURE 6

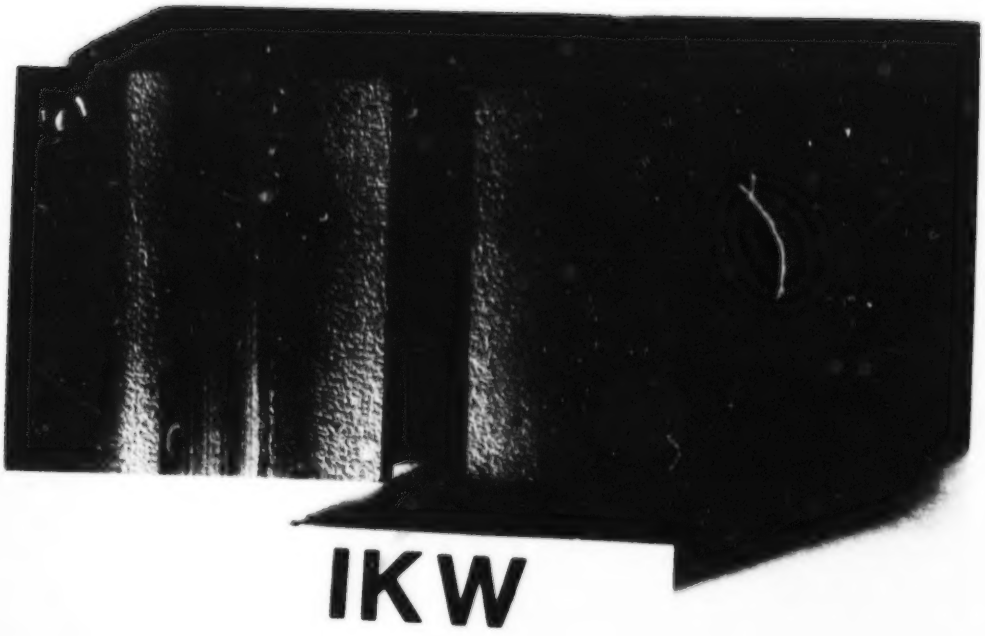

General Appearance of ERW K-55
Steel Coupons Provided by IPSCO

FIGURE 7

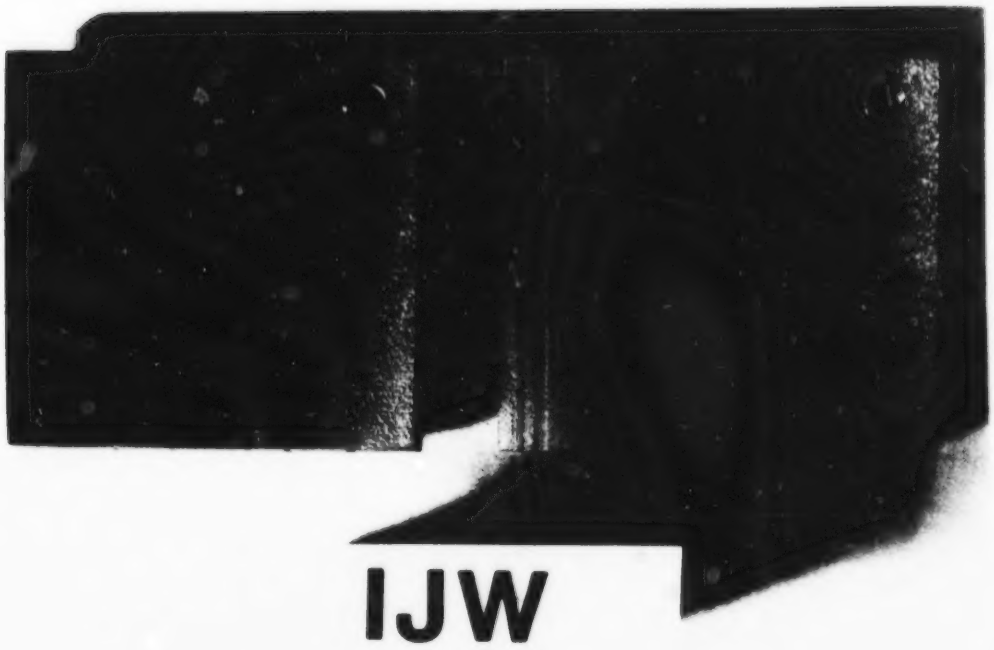

General Appearance of ERW J-55
Steel Coupons Provided by
IPSCO

FIGURE 8

General Appearance of ERW L80 Steel Coupons
Provided by IPSCO

FIGURE 9

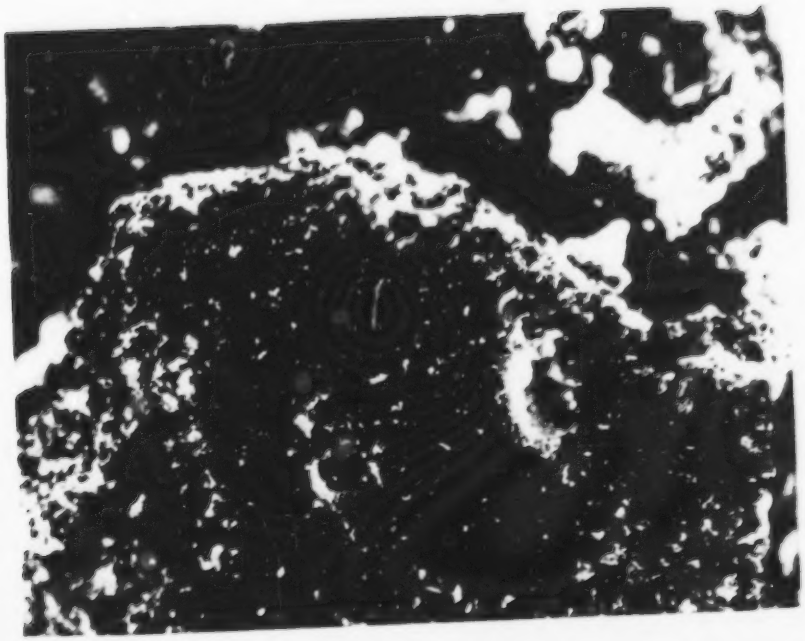

Coupon ILW17, photographed after Run 1, showing film found to consist mainly of pyrrhotite

Magnification x100

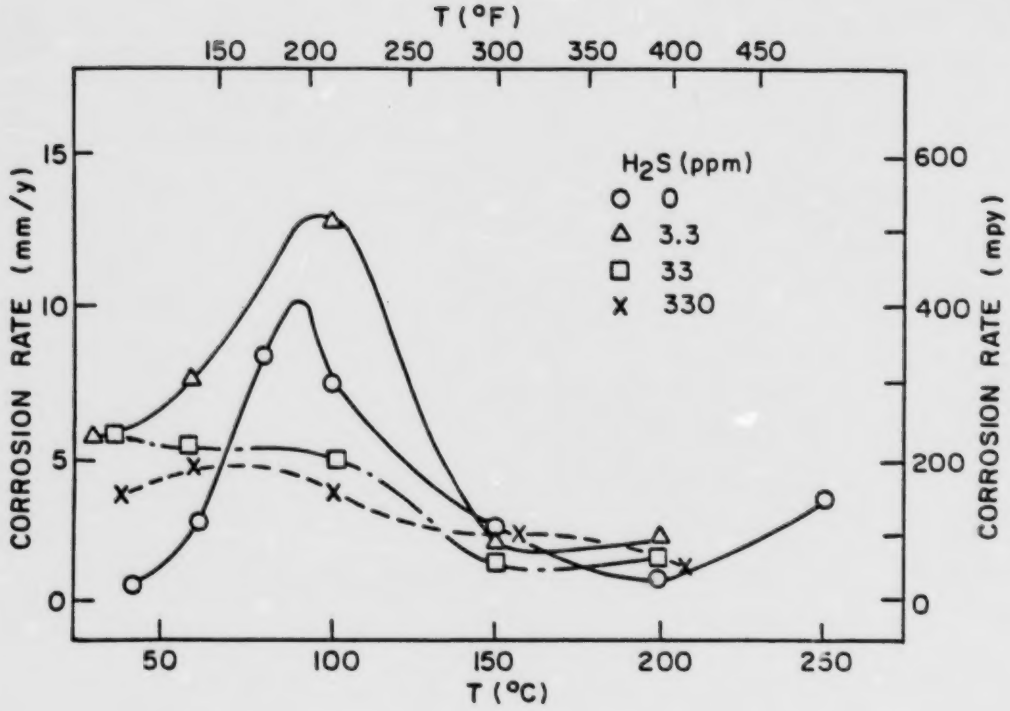

Fig. 10 Effect of H_2S and temperature on corrosion rate (pure iron) - (5% NaCl, 3.0 MPa $CO_2 + H_2S$ at 25 °C (77 °F); test duration, 96 h; flow velocity, 2.5 m/s; Specific volume, 25 cc/cm^2)

APPENDIX I

Results of Metallographic Examination

ORF

RESULTS OF METALLOGRAPHIC EXAMINATION

Test Run #1

Steel coupons from both Ipsco (K55, J55 and L80) and Algoma (K55, L80, and S0095) were exposed to test condition #1 (50% CO_2, 10% H_2S, 40% N_2, 4,000 psia total pressure) for 21 days. The exposed samples were examined for any form of corrosion in both polished and etched conditions. General surface attack, resulting from exposing the coupons to test condition #1, was the only form of corrosion observed. During the course of the metallographic examination, special attention was paid to the welded regions of the Ipsco steel coupons. However, no preferential corrosion attack was found in the welded region.

Detailed metallographic examinations were also performed on other grades of Ipsco (J55 and L80) and Algoma (L80 and S0095) steels which had been exposed to test condition #1. General corrosion was identified in all the test coupons.

Test Run #2

In test run #2, the concentration of H_2S was increased (50% CO_2, 50% H_2S, 4,000 psia, 150^{o}C for 13 days).

The measured corrosion rates, on both Ipsco (K55, J55 and L80) and Algoma (K55, L80 and S0095) steel coupons exposed to test condition #2, were higher than those measured on coupons exposed to test condition #1. Despite the fact that a higher corrosion rate was measured, the metallographic examination did not reveal any corrosion other than general surface attack on the steel coupons.

Test Run #3

The test run conditions of run #2 were similar to those of test #2 (50% CO_2, 50% H_2S, 150^{o}C, 4,000 psia, for 13 days), with the exception that ASTM D 1141 brine was the solution. In comparison with the measured corrosion rates in run #2, the presence of the bicarbonate, resulted in a lower corrosion rate for both Ipsco (K55, J55 and L80) and Algoma (K55, L80, S0095) steels, in run #3.

ORB

A preliminary metallographic examination of coupons exposed to test condition #3, showed the presence of surface cracks. These surface cracks were not observed in the steel coupons exposed to both test conditions #1 and #2. Metallographic examination was performed on the "as-received" steel coupons for runs #3 and #4. The surface cracks were also found on these unexposed samples. The origin of these cracks is not known.

Test Run #4

Test #4 (50% H_2S, 50% CO_2, 13 days, 4,000 psia, bicarbonate) is comparable to test condition #3, with the exception that the test temperature was lowered to 100°C. The results of the metallurgical examination on the Ipsco (K55, J55 and L80) and Algoma (L80 and S0095) steels which had been exposed to test run #4, are similar to those of test run #3. Essentially, only general corrosion was found on the surfaces of the above materials.

0692k

ORE

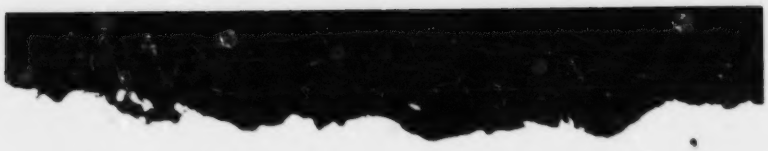

12.5 µm

Fig.1 Polished surface of a section of an 'as received' K55 (Algoma) steel coupon.

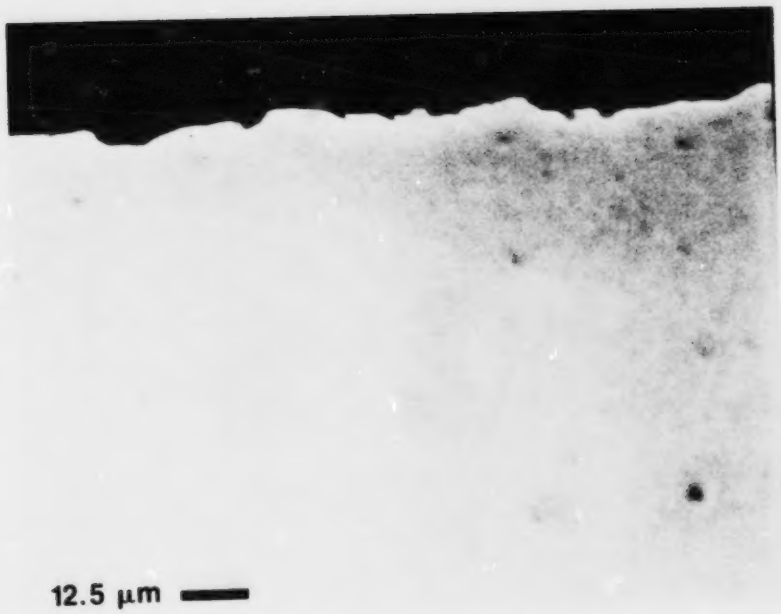

Fig.2 Polished surface of a section of an 'as received' K55 (Ipsco) steel coupon.

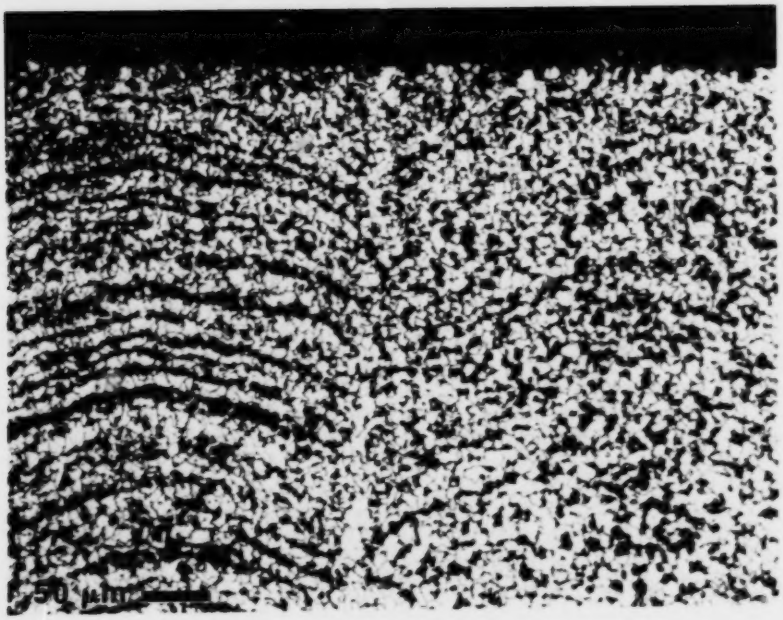

Fig.3 Etched surface of a section of an 'as received' K55 (Ipsco) steel coupon, showing the welded region.

12.5 µm

Fig.4 Polished surface of a section of a K55 (Ipsco) steel coupon, which had been exposed to test condition #1.

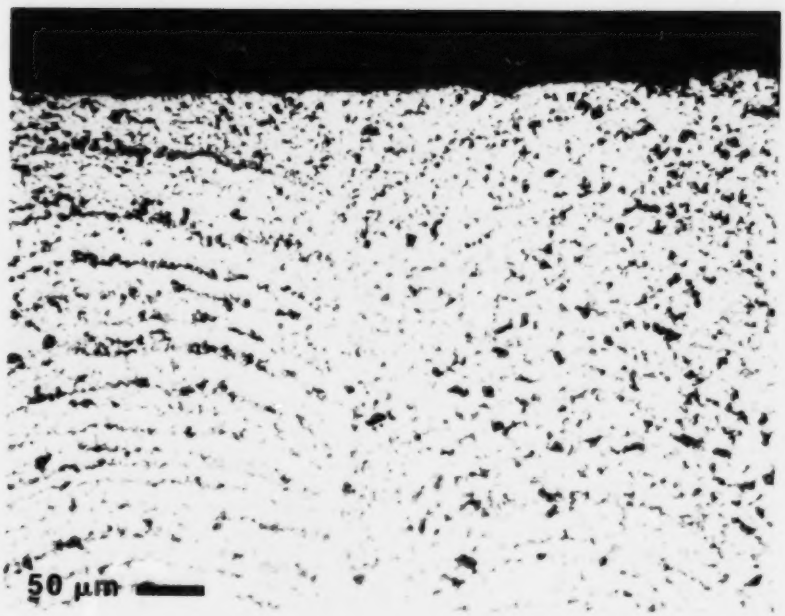

Fig.5 Etched surface of a section of a K55 (Ipsco) steel coupon, which had been exposed to test condition #1.

12.5 μm

Fig.6 A polished surface of a K55 (Algoma) steel coupon, which had been exposed to test condition #1.

12.5 µm

Fig.7 Surface of a polished section of a K55 (Algoma) steel coupon, which had been exposed to test condition #2.

12.5 µm

Fig.8 Polished surface of a section of K55 (Ipsco) steel coupon, which had been exposed to test condition #2.

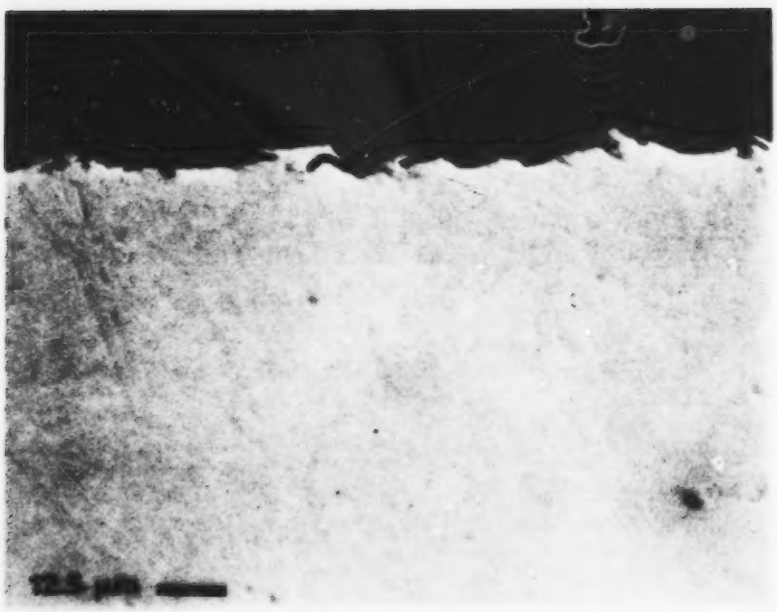

Fig.9 Polished surface of a section of L-80 (Ipsco) steel coupon in the as-received condition.

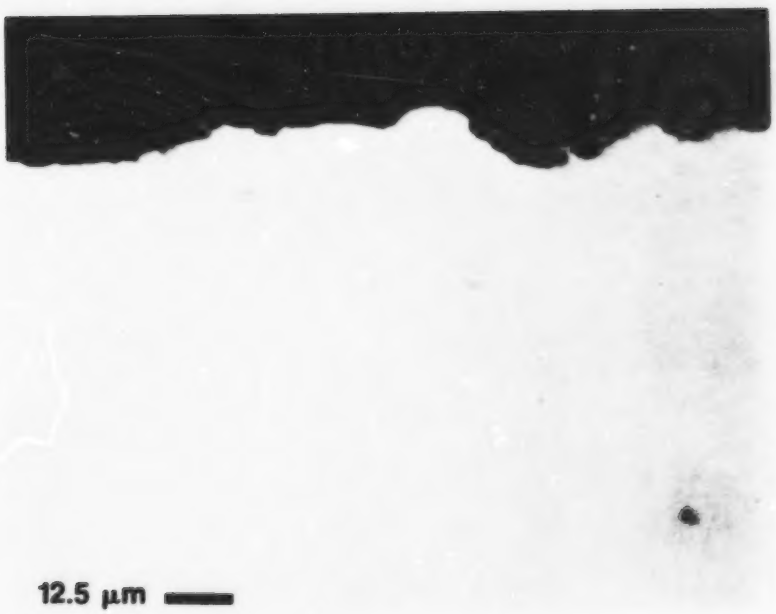

Fig.10 Polished surface of a section of L-80 (Ipsco) steel coupon which had been exposed to test condition #2.

12.5 µm

Fig.11 Polished surface of a K55 (Ipsco) steel coupon, which had been exposed to test condition #3.

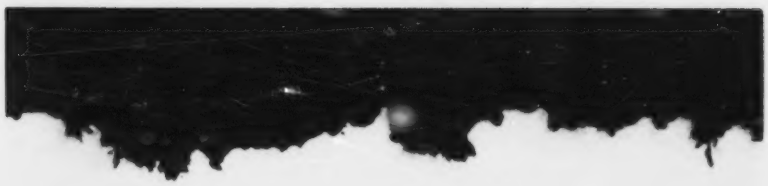

12.5 µm

Fig.12 Polished surface of a K55 (Algoma) steel coupon, which had been exposed to test condition #3.

12.5 μm

Fig.13 Polished surface of a section of an 'as received' K55 (Ipsco) steel coupon.

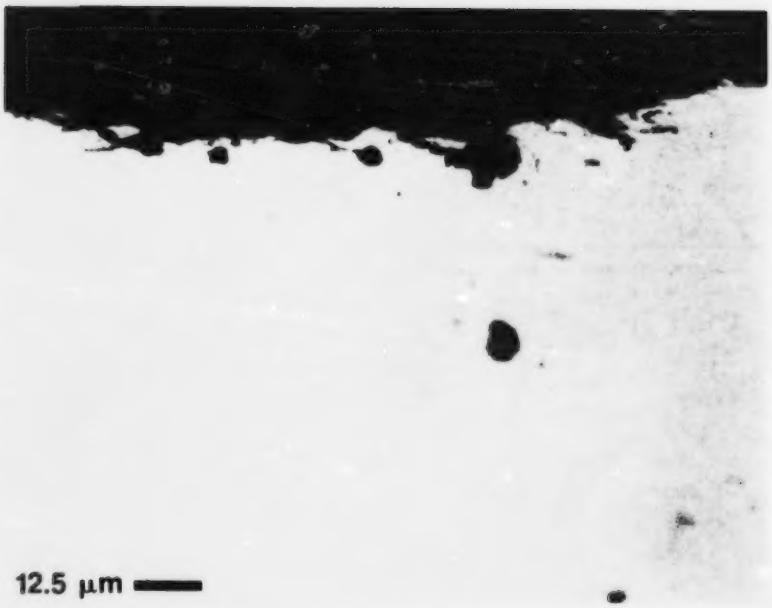

Fig.14 Polished surface of a section of an 'as received' K55 (Algoma) steel coupon.

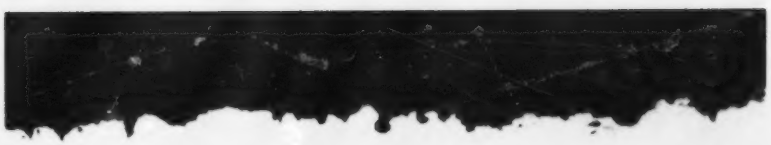

12.5 µm

Fig.15 A polished surface of a section of K55 (Ipsco) steel coupon, which had been exposed to test condition #4.

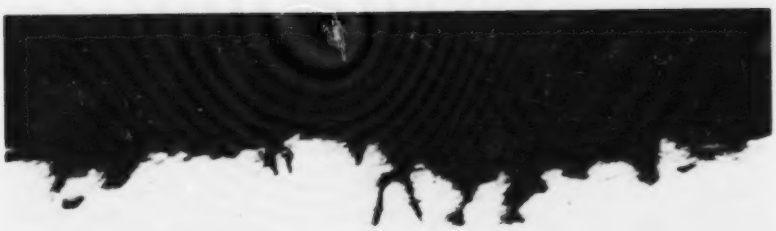

12.5 µm

Fig.16 A polished surface of a section of K55 (Algoma) steel coupon, which had been exposed to test condition #4.